iScience

CellPress
OPEN ACCESS

Article

Fluvastatin mitigates SARS-CoV-2 infection in human lung cells

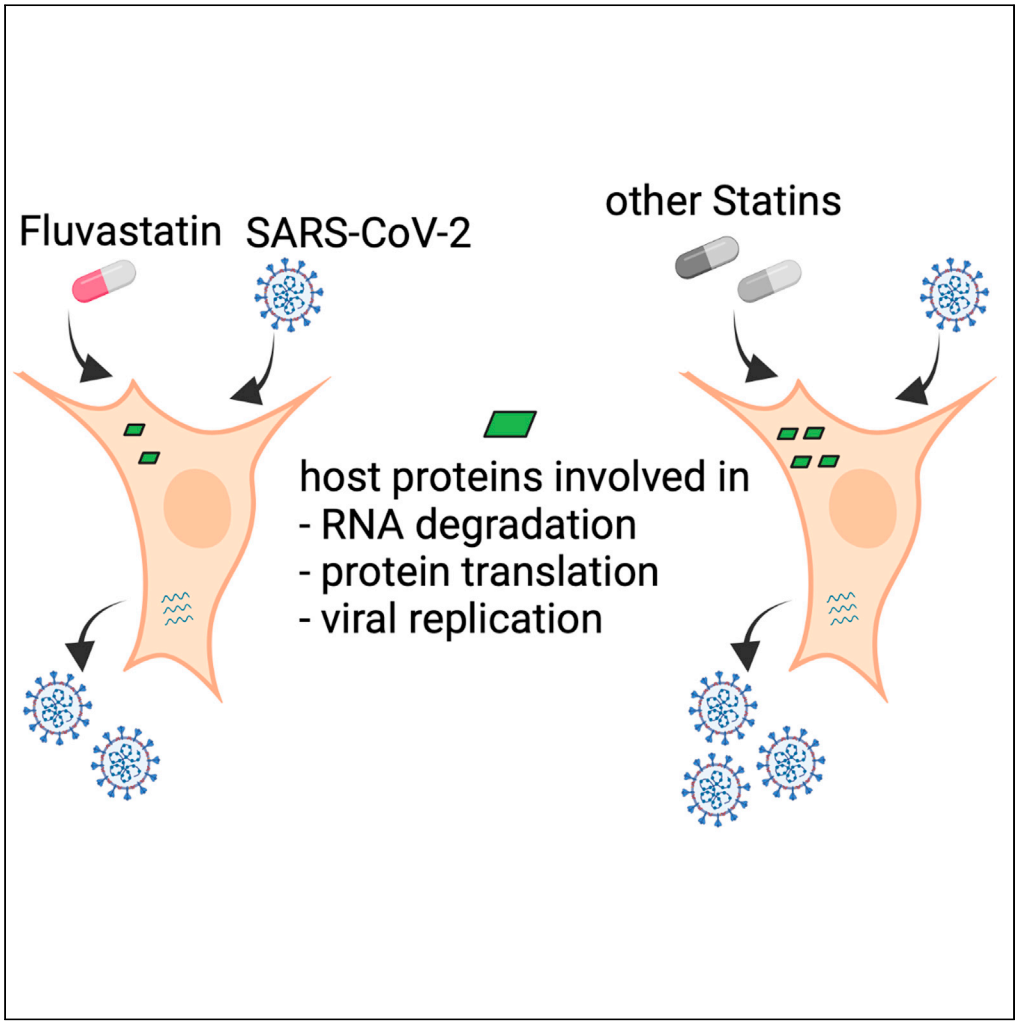

Francisco J. Zapatero-Belinchón, Rebecca Moeller, Lisa Lasswitz, ..., Anna K. Överby, Lothar Jänsch, Gisa Gerold

gisa.gerold@tiho-hannover.de

Highlights

Fluvastatin inhibits low (HCoV-229E) and high (SARS-CoV-2) pathogenic coronaviruses

SARS-CoV-2 infection does not affect statin-induced cholesterol biosynthesis arrest

Statin treatment does not alter SARS-CoV-2 innate immune responses *in vitro*

Fluvastatin downregulates protein translation and viral replication pathways

Zapatero-Belinchón et al., iScience *24*, 103469
December 17, 2021
https://doi.org/10.1016/j.isci.2021.103469

iScience

CellPress
OPEN ACCESS

Article

Fluvastatin mitigates SARS-CoV-2 infection in human lung cells

Francisco J. Zapatero-Belinchón,[1,2,3,4,9] Rebecca Moeller,[1,4,9] Lisa Lasswitz,[1,4,9] Marco van Ham,[5] Miriam Becker,[1,2,3] Graham Brogden,[1,4] Ebba Rosendal,[2,6] Wenjie Bi,[5] Belén Carriquí-Madroñal,[1,4] Koushikul Islam,[2,3] Annasara Lenman,[2,3] Antonia P. Gunesch,[1,7,8] Jared Kirui,[1,4] Thomas Pietschmann,[1,8] Anna K. Överby,[2,6] Lothar Jänsch,[5] and Gisa Gerold[1,2,3,4,10,*]

SUMMARY

Clinical data of patients suffering from COVID-19 indicates that statin therapy, used to treat hypercholesterolemia, is associated with a better disease outcome. Whether statins directly affect virus replication or influence the clinical outcome through modulation of immune responses is unknown. We therefore investigated the effect of statins on SARS-CoV-2 infection in human lung cells and found that only fluvastatin inhibited low and high pathogenic coronaviruses *in vitro* and *ex vivo* in a dose-dependent manner. Quantitative proteomics revealed that fluvastatin and other tested statins modulated the cholesterol synthesis pathway without altering innate antiviral immune responses in infected lung epithelial cells. However, fluvastatin treatment specifically downregulated proteins that modulate protein translation and viral replication. Collectively, these results support the notion that statin therapy poses no additional risk to individuals exposed to SARS-CoV-2 and that fluvastatin has a moderate beneficial effect on SARS-CoV-2 infection of human lung cells.

INTRODUCTION

Severe acute respiratory syndrome coronavirus 2 (SARS-CoV-2), the causative agent of coronavirus disease 2019 (COVID-19), has infected millions of people worldwide ("World Health Organization. Coronavirus Disease (COVID-19) Pandemic," 2020). Evidently, there are interindividual differences in the course of COVID-19 (Price-Haywood et al., 2020). Although higher age is a clear risk factor for severe disease, it remains largely elusive if premedication contributes to interindividual differences of COVID-19. A significant proportion of the population takes statins, in particular the elderly (Gu et al., 2014), who are at high risk of developing severe symptoms upon SARS-CoV-2 exposure (Davies et al., 2020). Although three independent retrospective studies report a correlation of statin therapy and reduced all-cause mortality of COVID-19 patients (Gupta et al., 2021; Masana et al., 2020; Zhang et al., 2020a), a large, observational, multicenter study does not confirm this notion (Mitacchione et al., 2021). In addition, statins may modulate expression of the angiotensin-converting enzyme 2 (ACE2) (Hoffmann et al., 2020a), receptor of SARS-CoV-2 and thus could impact infection (Li et al., 2013a; Shin et al., 2017). ACE2 is localized in lipid rafts, which are cholesterol- and glycosphingolipid-enriched microdomains of the plasma membrane (Li et al., 2007; Lu et al., 2008; Radenkovic et al., 2020). As statins are cholesterol-lowering drugs prescribed to treat hypercholesterolemia, cardiovascular disease, and diabetes, they may affect ACE2 microdomain localization and hence SARS-CoV-2 susceptibility. In addition, statins have pleotropic effects that may ameliorate COVID-19 (Ganjali et al., 2020; Liao and Laufs, 2005; Oesterle et al., 2017; Parsamanesh et al., 2021), including induction of nitric oxide (Laufs et al., 1998), reduction of reactive oxygen species (Wassmann et al., 2001), decreased numbers of inflammatory cells and inflammatory activity, and diminished serum levels of C-reactive protein and interleukin-6 (IL-6) (Bonsu et al., 2015). Moreover, statins may stabilize atheroma plaques by preventing oxidation of low-density lipoprotein (LDL) and recruitment of macrophages (Aviram et al., 1992; Crisby et al., 2001) and reduce thrombosis, most likely by reduction of tissue factor expression (Colli et al., 1997). Here we aim to understand whether statins influence disease outcome by directly impacting SARS-CoV-2 infection. To that end, we first investigated the role of statins on low pathogenic human coronavirus 229E infection. Then, we validated our findings with SARS-CoV-2 in cell lines and air-liquid interface cultures from differentiated human primary bronchial epithelial cells. Our

[1]Institute for Experimental Virology, TWINCORE, Centre for Experimental and Clinical Infection Research, A Joint Venture Between the Medical School Hannover and the Helmholtz Centre for Infection Research, 30625 Hannover, Germany

[2]Department of Clinical Microbiology, Virology, Umeå University, 90185 Umeå, Sweden

[3]Wallenberg Centre for Molecular Medicine (WCMM), Umeå University, 90185 Umeå, Sweden

[4]Department of Biochemistry & Research Center for Emerging Infections and Zoonoses (RIZ), University of Veterinary Medicine Hannover, 30559 Hannover, Germany

[5]Cellular Proteome Research Group, Helmholtz Centre for Infection Research, 38124 Braunschweig, Germany

[6]The Laboratory for Molecular Infection Medicine Sweden (MIMS), R893+F4 Umeå, Sweden

[7]Department of Gastroenterology, Hepatology and Endocrinology, Hannover Medical School, 30625 Hannover, Germany

[8]German Centre for Infection Research (DZIF), Partner site Hannover-Braunschweig, 30625 Hannover, Germany

[9]These authors contributed equally

[10]Lead contact

*Correspondence: gisa.gerold@tiho-hannover.de

https://doi.org/10.1016/j.isci.2021.103469

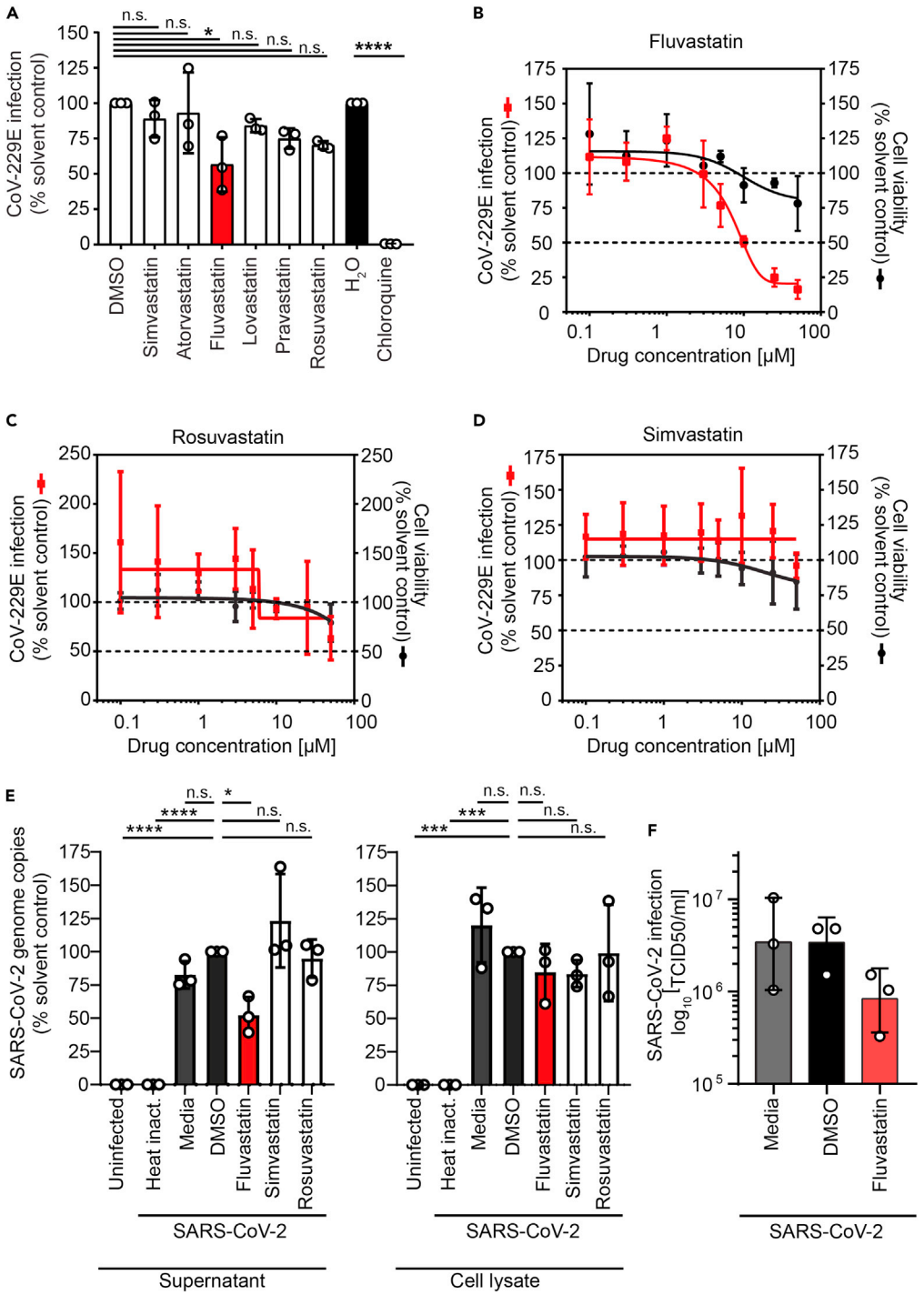

Figure 1. Lipid-lowering drugs selectively reduce coronavirus infection in human cells

(A) Huh7.5 Fluc cells were pretreated 24 h with the indicated statins (5 μM) or chloroquine as positive control and then infected with HCoV-229E harboring a Renilla reporter gene (MOI 0.005) in the presence of the drugs. Renilla luciferase activity as a measure of infectivity was determined 48 h after infection. The HCoV-229E infectivity (Renilla luciferase activity) was normalized to cell viability measured by the constitutive expression of Firefly luciferase in Huh7.5 Fluc cells. (B–D) Dose-response curves for the antiviral and cytotoxic effect of fluvastatin (B), rosuvastatin (C), and simvastatin (D) in Huh7.5 Fluc cells. Infection and statin treatment was performed as in (A) at the indicated statin concentration. The dotted lines indicate 100% and 50% infection and viablity.

Figure 1. *Continued*

(E) Fluvastatin decreases SARS-CoV-2 susceptibility of human respiratory epithelial Calu-3 cells. Virus genome copy numbers in cell lysates and supernatants from cells pretreated with selected statins (10 μM) or DMSO solvent control and infected with SARS-CoV-2 (MOI 2.0x10^{-5}) are shown. Results are normalized to viral copy numbers in DMSO-treated cells. (F) Number of infectious SARS-CoV-2 particles in cell culture supernatant from fluvastatin pretreated and SARS-CoV-2-infected Calu-3 cells (as in E) was determined by titration on Vero cells. (A–F) Mean ± SD of three independent biological replicates shown. One-way ANOVA, followed by Dunnett's multiple comparison test *p < 0.05, ***p < 0.0005, ****p < 0.0001.

study uncovered a dose-dependent reduction of susceptibility to SARS-CoV-2 by fluvastatin. To gain a systems biology understanding of the combined effect of statin treatment and SARS-CoV-2 infection on respiratory epithelium, we quantified global proteome changes and identified affected cellular networks. Statin treatment upregulated cholesterol synthesis enzymes in uninfected and infected cells. Moreover, innate immune sensing of the virus remained unaltered upon statin treatment. Interestingly, fluvastatin treatment uniquely affected the proteome signature of SARS-CoV-2-infected cells, specifically downregulating pathways and proteins important for RNA degradation, protein translation, and viral replication.

RESULTS

Selected statins reduce coronavirus infection in human cells

To assess a possible direct impact of statins on coronavirus infection, we infected Huh7.5 cells expressing a Firefly luciferase (Huh7.5 Fluc) with the low pathogenic human coronavirus 229E (HCoV-229E) in the presence of statins. At a concentration of 5 μM, statins reduced infection of HCoV-229E moderately between 10% and 40%. This inhibition was most pronounced (40%) and statistically significant for fluvastatin (Figure 1A). The most commonly prescribed statins, simvastatin and atorvastatin, reduced HCoV-229E infection up to 10%. Although lovastatin, pravastatin, and rosuvastatin reduced HCoV-229E infection up to 15%, 25%, and 30%, respectively, the observations did not reach statistical significance in the cell culture assay. Chloroquine completely blocked HCoV-229E infection as expected (Vincent et al., 2005; Wang et al., 2020). Detailed analysis revealed a dose-dependent reduction of coronavirus infection by fluvastatin with a half-maximal inhibitory concentration (IC_{50}) of 9.8 μM. At the investigated fluvastatin doses, cell viability remained at 80% and higher, indicating no major cytotoxic effects (Figure 1B). Dose-response analysis for rosuvastatin showed a 40% reduction of HCoV-229E infection at 50 μM, which correlated with a decrease in cell viability (Figure 1C). We did not observe a dose-dependent reduction of HCoV-229E infection upon simvastatin treatment (Figure 1D).

To investigate whether statins could modulate infection with highly pathogenic SARS-CoV-2, we pretreated human respiratory epithelial cells with 10 μM fluvastatin, rosuvastatin, or simvastatin and infected the cells with SARS-CoV-2 (strain SARS-CoV-2/München-1.2/2020/984,p3) (Wölfel et al., 2020). SARS-CoV-2 genome copy numbers significantly decreased to 60% in the supernatant upon fluvastatin treatment, whereas rosuvastatin or simvastatin treatment did not reduce SARS-CoV-2 genome copy numbers (Figure 1E). In cell lysates of infected cells treated with fluvastatin, rosuvastatin, or simvastatin, a slight reduction of about 15% of SARS-CoV-2 genome copy numbers was detected but did not reach statistical significance (Figure 1E). As we detected a significant decrease in SARS-CoV-2 genome copy numbers in supernatants upon fluvastatin treatment, we titrated released infectious SARS-CoV-2 particles. Fluvastatin treatment reduced SARS-CoV-2 titers 4-fold compared with DMSO treatment, as determined by TCID50 assay on Vero cells (Figure 1F). Collectively, our data highlight that statins do not promote coronavirus infection in human cells as was speculated, but instead selected statins attenuate coronavirus infection *in vitro*.

Fluvastatin moderately decreases SARS-CoV-2 infection in air-liquid interface cultures of human primary bronchial epithelial cells

We next aimed to corroborate our findings for fluvastatin treatment in a model that closely resembles the human respiratory tract. To that end, we differentiated human primary bronchial epithelial cells (HBECs) isolated from three different donors at an air-liquid interface (ALI) into a pseudostratified, polarized epithelium containing an apical layer of fully functional secretory and ciliated cells and an underlying layer of basal cells. SARS-CoV-2 infection was assessed in these ALI cultures with or without fluvastatin (10 μM or 50 μM), administered in the basolateral medium. Here, we increased the dosage of fluvastatin above the IC_{50}

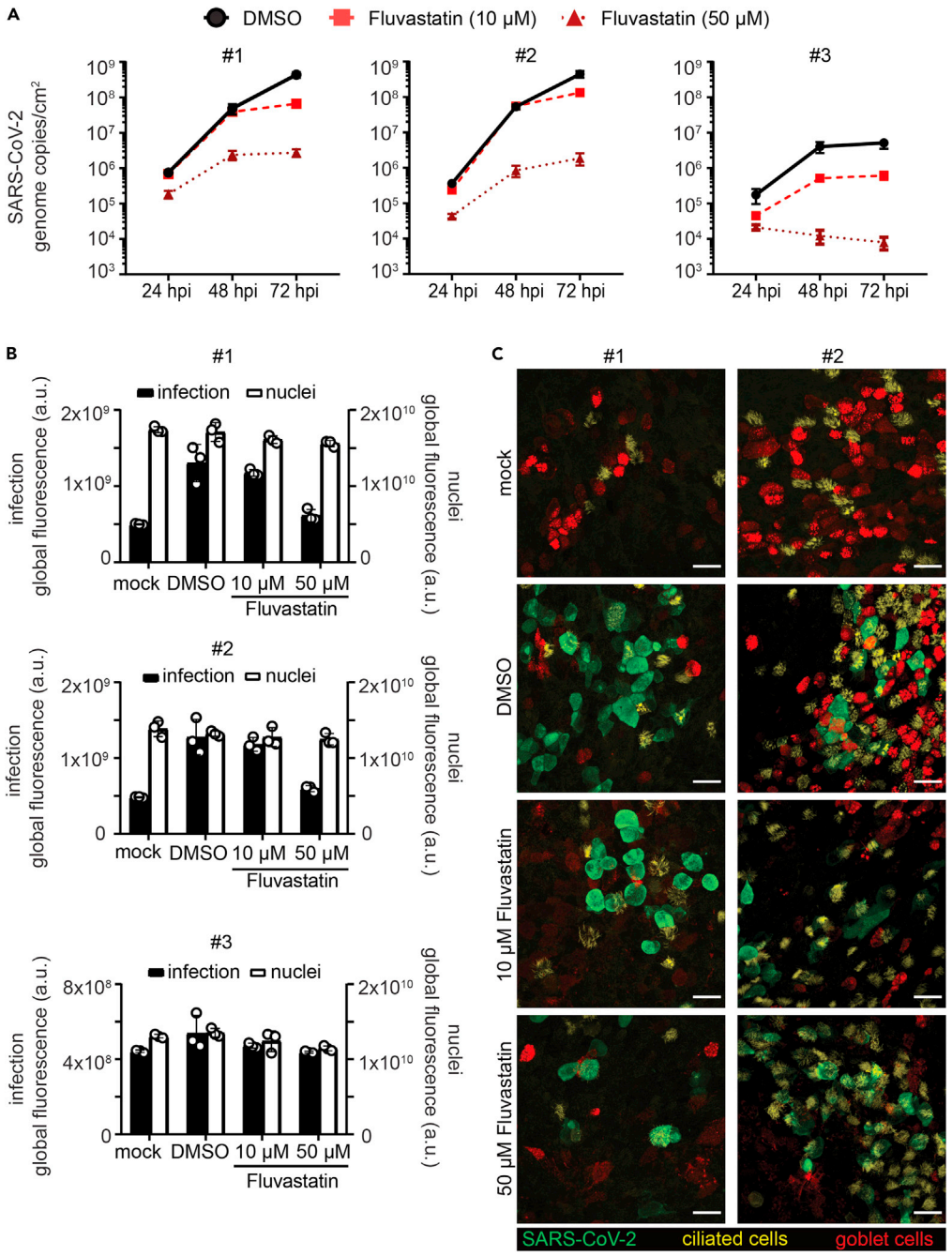

Figure 2. Fluvastatin treatment reduces SARS-CoV-2 infection in HBEC ALI cultures

(A–C) HBEC ALI cultures from three donors were pretreated with DMSO solvent control or fluvastatin (10 μM or 50 μM) in the basal media for 24 h prior to SARS-CoV-2 infection at the apical side (4.5×10^4 PFU). (A) To assess viral replication, apical samples from HBEC ALI cultures were collected 24, 48, and 72 h postinfection by a 1-h wash in 300 μL growth medium. Progeny virus released within these 24 h periods were quantified by real-time q-PCR alongside an RNA standard. RNA genomes per ALI area in DMSO-treated samples (circle, black solid line) was plotted against time for the different statin concentrations (10 μM: square, red dashed line; 50 μM: triangle, dark red dotted line). Real-time q-PCRs were run in duplicates from three HBEC ALI inserts per sample. Data shown as mean of three biological replicates ± SEM. (B) ALI cultures were fixed at 72 h (endpoint) and stained for SARS-CoV-2 nucleocapsid protein and nuclei and analyzed by immunofluorescence. Global fluorescence intensity of infection (black bars) and nuclei (white bars) was quantified from a fixed ROI omitting the well borders. Depicted are averages and SD in global fluorescence in arbitrary units from triplicates

Figure 2. *Continued*
per condition from HBEC ALIs for each donor. (C) ALI samples at 72 h (endpoint) were stained for SARS-CoV-2 nucleocapsid protein for infection (green), mucin5AC for secretory cells (red) and acetylated tubulin for ciliated cells (yellow) and imaged on a scanning confocal microscope. Depicted are maximum intensity projections from z-stacks of representative sites for the different conditions from two different individuals. Scale bars, 25 μm.

determined in monolayer cell culture, as in this more complex multilayer cell culture model higher doses might be required.

To monitor the course of infection, we measured progeny virus release into the apical mucus with real-time qPCR in 24 h intervals. Viral RNA pronouncedly increased over 72 h ($7x10^5$ to $4x10^8$ for donor #1; $3x10^5$ to $4x10^8$ for donor #2; and $1x10^5$ to $5x10^6$ for donor #3; Figure 2A black lines), indicating active viral replication in the ALI cultures. We detected varying levels of viral RNA in the samples from different donors (donor #1 and #2 *vs.* donor #3), which may reflect differences in susceptibility of individuals as observed in natural infection. Treatment with 10 μM fluvastatin did not affect viral release in highly infected samples (donor #1 and #2; Figure 2A, red dashed lines), whereas a moderate decrease in released virus was observed in a less infected sample ($6x10^5$ to $5x10^6$ in donor #3; Figure 2A, red dashed line). In contrast, treatment with 50 μM fluvastatin dramatically reduced viral release in samples from all donors (at least two log steps, Figure 2A, dark red dotted lines).

We next immunostained the HBEC ALI cultures for differentiation markers of ciliated cells (acetylated tubulin, Figure 2C, yellow) and goblet cells (mucin5AC, Figure 2C, red) in addition to SARS-CoV-2 nucleocapsid protein (SARS-CoV-2 NC) (Figure 2C, green) and acquired overview images of all samples (Figure S1), as well as detailed confocal images of highly infected HBEC ALI cultures (donor #1 and #2; Figure 2C). We observed differences in number of goblet and ciliated cells between the donors, which may reflect donor-dependent cell-type variation or slight differences in the differentiation. SARS-CoV-2 infection was mainly detected in ciliated cells as reported previously for ALI cultures (Ravindra et al., 2020), but also in unstained cell populations, that most possibly represent basal cells or differentiation intermediates as reported for human lung tissues (Hui et al., 2020).

To validate our findings, we quantified the intracellular infection levels by immunofluorescence staining for SARS-CoV-2 NC on the HBEC ALI cultures at 72 h. Sample integrity was assessed at the same time by nuclear staining. We observed that the nuclear signal remained constant upon infection or fluvastatin treatment for all samples (Figure 2B, white bars), indicating no cellular loss upon treatment and infection. SARS-CoV-2 NC positive cells appeared at many sites in the cultures for the highly infected samples from donor #1 and donor #2, whereas the samples from donor #3 showed only a few sites with SARS-CoV-2 NC positive cells (Figure 2B, black bars, DMSO and Figure S1), in line with the number of virus particles released in the supernatant. Fluvastatin treatment reduced the overall SARS-CoV-2 NC signal only slightly at lower dose (Figure 2B, black bars, 10 μM and Figure S1) and strongly at the higher dose (Figure 2B, black bars, 50 μM and Figure S1).

In summary, these results suggest that fluvastatin treatment has a moderate attenuating effect in SARS-CoV-2-infected three-dimensional epithelium cell culture models as seen in the monolayer system.

Statins regulate cholesterol synthesis independently of SARS-CoV-2 infection

To determine the effects of fluvastatin, rosuvastatin, and simvastatin on global cellular processes (e.g. cholesterol biosynthesis), we pretreated Calu-3 cells with either indicated statins or solvent control followed by mock (uninfected) or SARS-CoV-2 infection. Subsequently, we analyzed cellular proteomes by label-free mass spectrometry (Figure 3A). We additionally incubated Calu-3 cells with heat-inactivated virus to control for changes in the cellular proteome induced by noninfectious particle exposure. All experiments were performed in biological triplicates, generating quantitative information of 27 proteomes in total. In line with our previous experiments, SARS-CoV-2 genome copies decreased in supernatants of fluvastatin-treated cells compared with DMSO-treated cells (Figure S2A). In total, 3,229 proteins were identified unambiguously by at least one unique tryptic peptide. Global inspection of our proteomic data revealed four cholesterol biosynthesis pathway enzymes that were significantly more abundant (either $-\log_{10}$(p value) $\geq$ 2 or $\log_2$(fold change) $\pm$ 4 and $-\log_{10}$(pvalue) $\geq$ 1.3) upon treatment with fluvastatin, namely 3-hydroxy-3-methylglutaryl-CoA reductase (HMGCR), farnesyl-diphosphate farnesyltransferase 1 (FDFT1), squalene

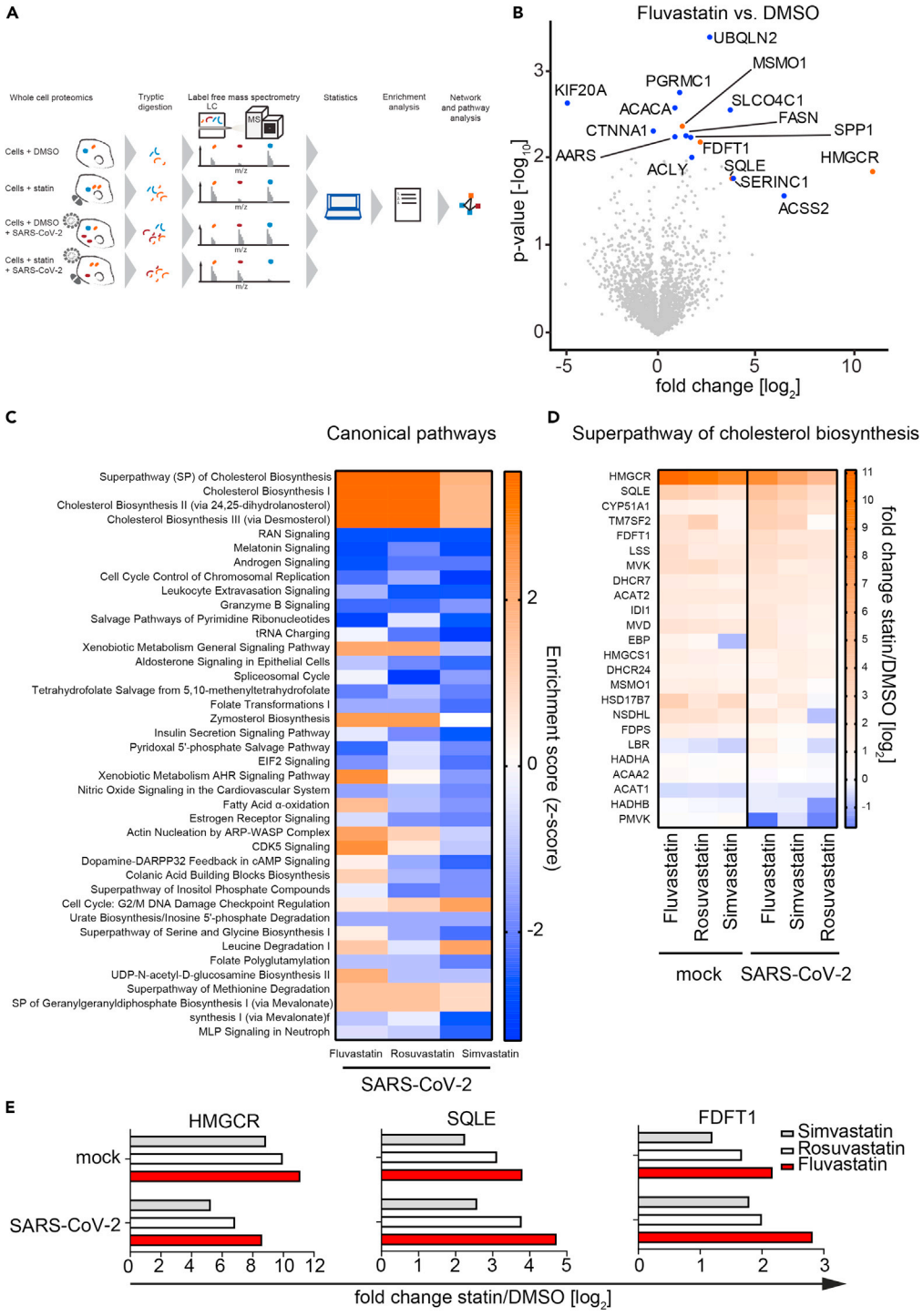

Figure 3. Statin treatment upregulates expression of proteins involved in cholesterol synthesis

(A) Experimental workflow of the whole-cell shotgun proteomics analysis. Three independent passages of Calu-3 cells were pretreated with 10 μM of the different statins or solvent control for 24 h and subsequently infected in the presence of the drug with SARS-CoV-2 (MOI $2.0x10^{-5}$) or left uninfected (mock). Forty-eight hours later, viral titer was determined via real-time qPCR from the supernatants (see Figure S2A), and cells were lysed and used for protein extraction and subsequent analysis by label-free mass spectrometry. Unambiguous tryptic peptides were identified, and protein abundance was determined by label-free quantification algorithms and compared between different experimental conditions.

Figure 3. *Continued*

(B) Volcano plot showing changes in protein abundance in fluvastatin-treated cells versus DMSO solvent-control-treated cells. Significantly enriched proteins (either –log10 p value ≥ 2 or log2 fold change ≥ ±4 with –log10 p value ≥ 1.3) are highlighted in blue; significantly enriched proteins involved in the cholesterol synthesis pathway are highlighted in orange. n = 3; significance was analyzed using the Student's t test.

(C) Analysis of top 40 significantly enriched canonical pathways (p value ≤ 0.05) upon statin treatment in SARS-CoV-2-infected Calu-3 cells.

(D) Statin-induced changes in protein abundance in the superpathway of cholesterol synthesis in SARS-CoV-2-infected cells and uninfected cells (mock).

(E) Median intensity differences from three independent experiments of selected cholesterol synthesis pathway proteins upon indicated statin treatment. Experiments performed in biological triplicates.

monooxygenase (SQLE), and methylsterol monooxygenase 1 (MSMO1) (Figure 3B, shown in orange). In addition, expression levels of twelve proteins unrelated to cholesterol biosynthesis changed significantly (shown in blue). To further investigate the modulatory effects of each statin during SARS-CoV-2 infection, we compared the top 40 altered cellular pathways for each experimental condition. All three statins upregulated cholesterol biosynthesis pathways and depleted Ran, melatonin, and androgen signaling pathways (Figure 3C). The upregulation of cholesterol biosynthesis enzymes to antagonize statin-mediated blockade of HMGCR is in line with previous reports (Borthwick et al., 2014). Expectedly, statin treatment led to a slight decrease in cholesterol concentration in cells cultured in the absence of FCS, whereas no decrease in cholesterol was observed in cells cultured in medium containing FCS, as used in our experimental conditions (Figure S2B). Importantly, cholesterol synthesis proteins were upregulated in both the presence and absence of SARS-CoV-2 infection (Figure 3D). Specifically, HMGCR, SQLE, and FDFT1 expression levels increased upon treatment with fluvastatin, simvastatin, and rosuvastatin independently of SARS-CoV-2 infection (Figure 3E); this strongly suggests that SARS-CoV-2 infection itself does not impair statin-mediated cholesterol synthesis inhibition (Figures 3D and 3E).

Statin treatment does not impair the innate immune response against SARS-CoV-2

During SARS-CoV-2 infection, the innate immune response plays an important role in fighting the virus (Blanco-Melo et al., 2020). However, immune responses also cause the observed immunopathology in COVID-19 patients (Allegra et al., 2020). Therefore, it is crucial to assess how prescribed medications, such as statins, modulate host defense mechanisms in the context of SARS-CoV-2 infection. To that end, we compared protein expression levels in fluvastatin-treated uninfected cells with protein expression levels in fluvastatin-treated SARS-CoV-2-infected cells (Figure 4A). As expected, we found viral proteins such as the spike protein (S), the matrix protein (M) as well as the accessory protein 9b (Orf9b) in lysates from infected cells in all conditions (red dots in Figure 4A for fluvastatin treated conditions). In addition, virus infection in fluvastatin-treated cells upregulated host proteins such as the interferon-induced GTP-binding protein Mx1 (MX1), transcription termination factor 2 (TTF2), WD repeat-containing protein 87 (WDR87), and DENN domain containing 6A (DENND6A). Among the downregulated proteins upon infection were host proteins such as septin-8 (SEPT8) and nuclear-receptor-binding protein (NRBP1). We next analyzed which upstream regulators could account for the observed differences in protein abundance in uninfected and infected cells in the presence or absence of statins (Figure 4B). Here, we additionally included the protein abundance profiles of cells incubated with a heat-inactivated virus control to account for protein dysregulation caused by the inoculum in the absence of viral genome replication. Interestingly, we observed that tumor necrosis factor (TNF)-modulated proteins were strongly downregulated in infected cells treated with DMSO, simvastatin, or rosuvastatin, whereas fluvastatin treatment prevented this downregulation. In fact, SARS-CoV-2-infected cells pretreated with fluvastatin displayed similar TNF-modulated protein abundance patterns as cells inoculated with the heat-inactivated virus control. In contrast to the down-modulating effect on the TNF pathway, SARS-CoV-2 infection increased the expression of proteins regulated by interferon lambda-1 (IFNL1) and interferon alpha-2 (IFNA2). This IFN pathway induction occurred both in the absence and in the presence of all three statins (enrichment scores between 2 and 3), whereas it was absent in cells incubated with heat-inactivated virus control; this suggests that sensing of the virus in our cell culture system depends on active viral replication and that this sensing is not largely impaired by statins. Next, we examined the protein abundance of genes regulated by TNF, IFNL1, and IFNA2 in uninfected and infected cells (Figures 4C and 4D). SARS-CoV-2 infection downregulated TNF-dependent proteins such as heparan sulfate proteoglycan 2 (HSPG2) or syndecan 4 (SDC4) independent of statin treatment (Figure 4C). In contrast, virus infection strongly upregulated expression of the interferon-induced protein with tetratricopeptide repeats 3 (IFIT3) and IFIT1 in DMSO-, simvastatin-, and rosuvastatin-treated

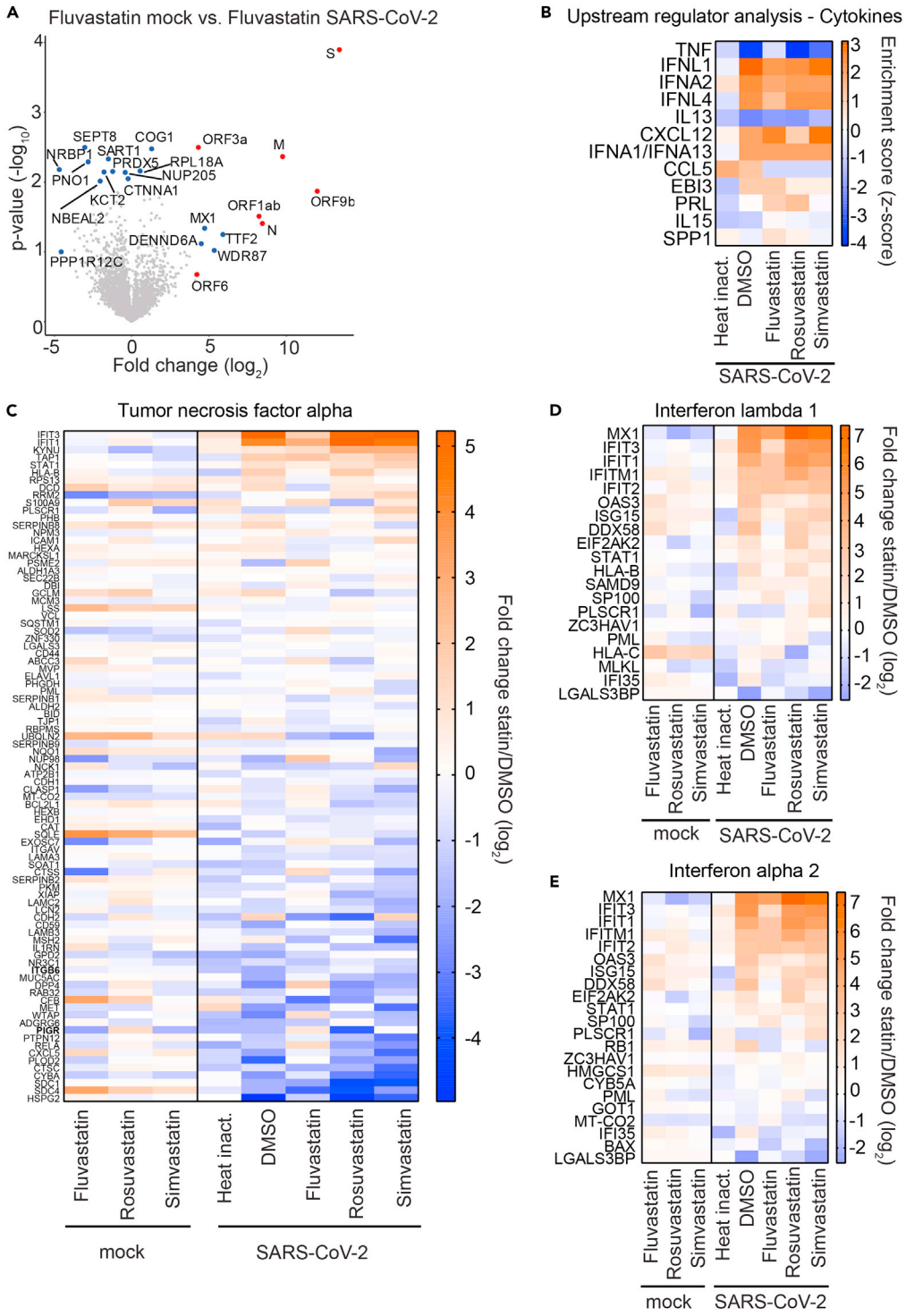

Figure 4. Statin treatment does not alter the innate immune response to SARS-CoV-2

(A) Volcano plot showing changes in cellular protein abundance upon SARS-CoV-2 infection of fluvastatin-treated cells. Viral proteins are depicted in red and significantly modulated host proteins in blue (either –log10 p value ≥2 or log2 fold change ≥ ±4 with –log10 p value ≥1.3). n = 3; significance was analyzed using the Student's t test.

(B) Heatmap showing upstream regulatory cytokines and chemokines affecting protein abundance in cells upon SARS-CoV-2 infection and statin treatment (red upregulated pathway; blue: downregulated pathway).

Figure 4. *Continued*
(C–E) Changes in TNF-regulated (C) and interferon-stimulated genes (D, E) upon SARS-CoV-2 infection and statin treatment. Heatmap representing the log2 fold change in protein abundance upon statin treatment as compared with the DMSO solvent control in uninfected (mock) or SARS-CoV-2-infected cells. Heat inact.: replication-deficient heat-inactivated virus control. Median intensities from three biological replicates.

cells, but not to the same degree in fluvastatin-treated cells. Indeed, fluvastatin-treated SARS-CoV-2-infected cells showed protein expression patterns of intermediate phenotype between heat-inactivated virus incubated cells and DMSO-treated SARS-CoV-2-infected cells. The interferon-inducible protein MX1 was downregulated in statin-treated uninfected cells compared with DMSO-treated uninfected cells but was highly induced upon SARS-CoV-2 infection (Figures 4D and 4E). Interestingly, we found that statin treatment upregulated the interferon-inducible proteins 2′-5′-oligoadenylate synthetase 3 (OAS3), ISG15 ubiquitin-like modifier (ISG15), DExD/H-box helicase 58 (DDX58), and major histocompatibility complex, class I, C (HLA-C) in uninfected cells. This suggests a possible modulatory role of statins on the innate immune response of the respiratory epithelium (Figures 4D and 4E). In the context of SARS-CoV-2 infection, DMSO, simvastatin, and rosuvastatin treatment did not strongly affect the antiviral innate immune response, but fluvastatin treatment slightly decreased innate immune responses to SARS-CoV-2 infection.

Fluvastatin induces a unique protein expression profile in SARS-CoV-2-infected cells compared with simvastatin and rosuvastatin

Our results suggest that fluvastatin may inhibit SARS-CoV-2 infection independently of its main cellular target HMGCR (Figure 3). To elucidate secondary fluvastatin-specific effects in SARS-CoV-2-infected cells, we compared protein expression levels in infected cells with and without statin treatment. To focus on highly regulated proteins, we included proteins with either a $-\log_{10}$(p value) $\geq$ 2 or with a $\log_2$(fold change) $\pm$ 4 and a $-\log_{10}$(p value) $\geq$ 1.3 in our analysis (Figure 5A). Eleven proteins were upregulated in infected cells treated with fluvastatin as compared with infected cells treated with DMSO. Expectedly, fluvastatin treatment upregulated HGMCR expression 380-fold over DMSO-infected cells. Seven host proteins, including the E3 ubiquitin ligase cullin CUL4B and the cytoskeletal forming GTPase SEPT8, were downregulated upon fluvastatin treatment. In addition, fluvastatin pretreatment reduced the expression of seven viral proteins, with ORF1ab, ORF3a, and ORF6 protein abundance being significantly reduced (Figure S3); this is in line with the observed reduced virus load as measured by real-time qPCR and plaque assay (Figures 1 and S2A). Next, we unbiasedly clustered protein expression levels of statin or DMSO-treated infected cells according to the differentially regulated pathways in each dataset (Figures 5B and S4). Strikingly, we found that fluvastatin-treated infected cells clustered independently from simvastatin-, rosuvastatin-, or DMSO-treated infected cells. This confirms that fluvastatin differentially affects the cellular proteome of SARS-CoV-2-infected cells. The cluster of pathways exclusively downregulated by fluvastatin included inhibition of ARE-mediated mRNA degradation, pyrimidine ribonucleotide *de novo* biosynthesis, telomerase signaling, PI3K/AKT signaling, protein kinase A signaling, and the unfolded protein response (Figure S4). Among the pathways exclusively upregulated by fluvastatin, we found systematic lupus erythematosus in T cell signaling, UDP-N-acetyl-D-galactosamine biosynthesis II, CDK5 signaling, and the spliceosomal cycle (Figure S4). These results suggest that fluvastatin-treated infected cells may display stronger mRNA degradation and spliceosomal turnover than DMSO-, simvastatin-, or rosuvastatin-treated infected cells.

To shed more light on the proteins specifically downregulated (p values < 0.05) by fluvastatin, but not simvastatin and rosuvastatin, in SARS-CoV-2-infected cells, we analyzed the differential abundance of proteins in infected cells treated with each statin in comparison to DMSO. Fluvastatin decreased the expression levels of 35 proteins, whereas simvastatin and rosuvastatin decreased the expression levels of 25 and 18 proteins in infected cells, respectively. Strikingly, we did not find any protein downregulated by all three statins. In addition, there was little overlap between pairs of two statins (Figure 5C), suggesting that statins differentially downregulate protein expression upon infection. In total, 29 of the 35 proteins downregulated by fluvastatin were specific to this statin. To determine whether these 29 proteins are interconnected, we performed STRING network analysis. We found two major clusters of interacting proteins in our dataset that were significantly enriched (PPI enrichment: 3.96×10^{-4}) (Figure 5D). The first cluster comprised four proteins and contained a mitochondrial protein involved in mitochondrial matrix peptide translocation (TIMM44) and a regulator of innate RNA recognition (TUFM). The second cluster comprised 15 proteins, most of which can be acetylated (12/15), have an isopeptide bond (10/15), or bind RNA (8/15) (compare

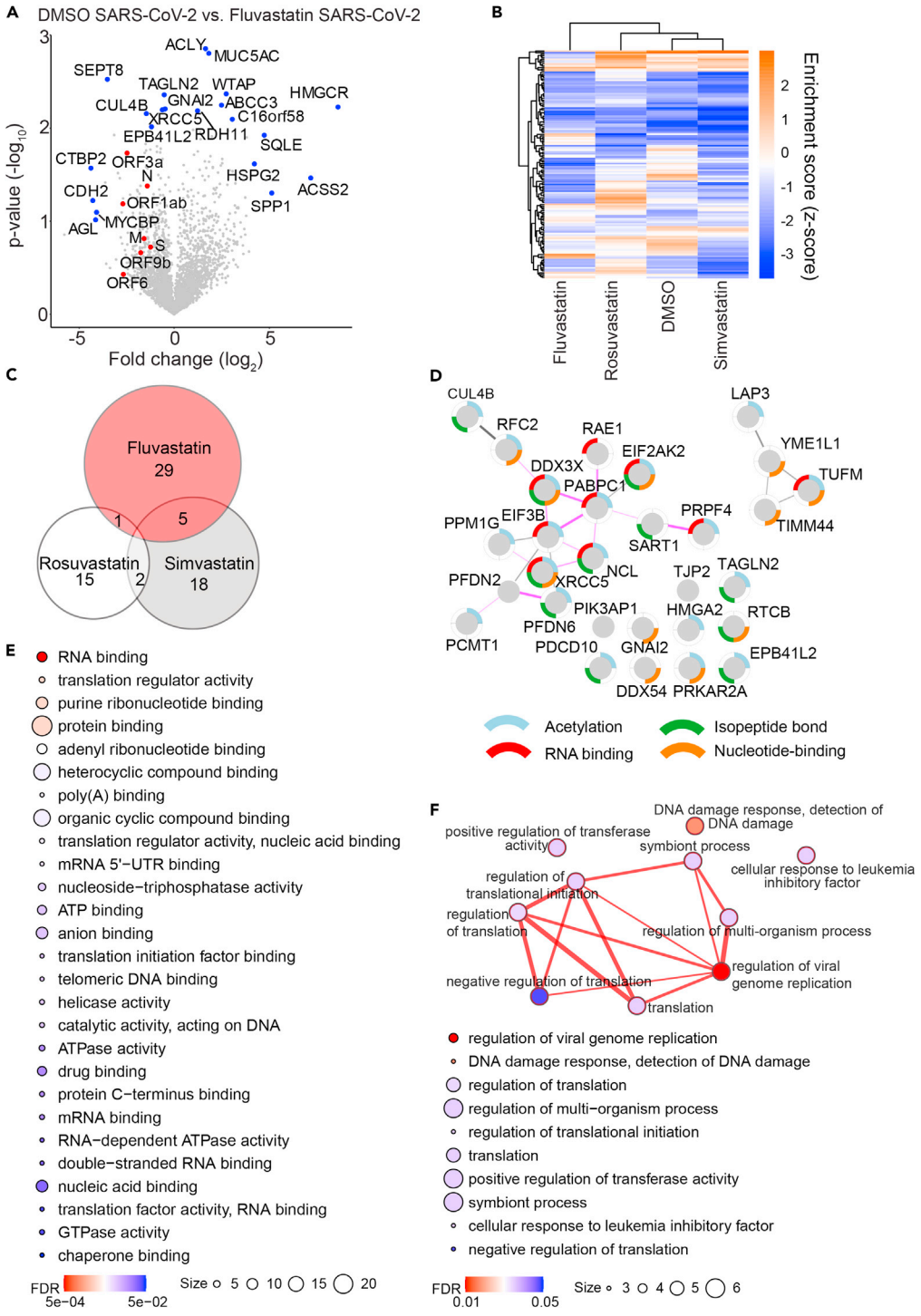

Figure 5. Fluvastatin induces a unique translational profile during SARS-CoV-2 infection

(A) Volcano plot showing fluvastatin-induced changes in cellular protein abundance in SARS-CoV-2-infected cells. Viral proteins shown in red and significantly modulated host proteins in blue (either –log10 p value ≥ 2 or log2 fold change ≥ ±4 with –log10 p value ≥ 1.3). n = 3; significance was analyzed using the Student's t test.

(B) Canonical pathway analysis of whole-cell proteome from SARS-CoV-2-infected cells with indicated treatments with (a)-log10 p value of at least 2. Hierarchical clustering based on enrichment scores. For a magnified heatmap including pathway information please refer to Figure S4.

Figure 5. *Continued*

(C) Venn diagram of proteins significantly downregulated in SARS-CoV-2-infected cells upon treatment with the indicated statins. Numbers indicate statin-specific and overlapping proteins for the indicated treatment.

(D) STRING network of proteins downregulated during SARS-CoV-2 infection in a fluvastatin-specific manner. Nodes represent proteins, and lines predicted interactions with line thickness, indicating the strength of evidence (pink lines: experimental evidence; gray lines: co-expression, text mining, co-occurrence, database). Node border colors indicate the top four enriched gene ontology terms as indicated.

(E) Enriched gene ontology functions from fluvastatin downregulated proteins. Circle size signifies number of proteins with the indicated function and color-calculated FDR value.

(F) (Top) Map depicting the enriched gene ontology biological processes within the dataset of fluvastatin downregulated proteins. Nodes represent biological process term and line thickness level of gene overlap between processes. Network node color displays FDR values. (Bottom) List of enriched biological process terms indicating number of proteins per term (size) and FDR values (color).

color-coding of the node border). Moreover, according to experimental evidence, most proteins in the second cluster interact with each other (13/15) (compare pink edges). Among these proteins we found the mRNA poly(A) tail binding protein polyadenylate-binding protein 1 (PAPBC1), the eukaryotic initiation factor 3 subunit B (EIF3B), the RNA helicase DEAD-Box helicase 3 X-Linked (DDX3X), and the IFN-induced protein kinase R (EIF2AK2, or PKR).

To determine if protein expression changes were a result of transcriptional regulation, we quantified transcript levels of selected downregulated proteins using qPCR in SARS-CoV-2-infected cells treated with statins (Figure S5). Fluvastatin or rosuvastatin treatment significantly reduced replication factor C subunit 2 (*RFC2*) mRNA levels in cells infected with SARS-CoV-2 as compared with the infected solvent-control-treated cells. In contrast, high-mobility group protein AT-Hook 2 (*HMGA2*) mRNA levels remained similar in all infected cells treated either with statins or DMSO, while nucleolin (*NCL*) transcript levels were significantly reduced only in cells treated with fluvastatin compared with the solvent control. These data partially reflect our proteomics data, suggesting that statins may act not only at the level of gene expression but also on protein translation and degradation.

Gene ontology analysis of the associated molecular functions of the downregulated proteins revealed, among others, enrichment of proteins involved in RNA binding (FDR = $5.4x10^{-4}$), translation regulator activity (0.0026), poly(A) binding (0.0057), and mRNA 5′-UTR binding (0.0074) (Figure 5E); this suggests that the proteins specifically downregulated in fluvastatin-treated SARS-CoV-2-infected cells play a role in translation regulation. When we compared the biological processes associated with all 29 proteins downregulated by fluvastatin in infected cells, we observed that the enriched biological processes are tightly interconnected (Figure 5F). Whereas most of the enriched biological processes were related to protein translation, the most significantly enriched gene cluster was annotated as regulation of viral genome replication (FDR = 0.0103) and contained *EIF2AK2, PABPC1, DDX3X*, and *HMGA2*. In sum, these findings suggest that the proteins specifically downregulated by fluvastatin in SARS-CoV-2-infected cells may play a role in protein translation and thus SARS-CoV-2 replication.

DISCUSSION

Considering that a significant fraction of the population, i.e. 26% of all Americans over the age of 40 years (Gu et al., 2014) and 30%–40% of all type 2 diabetes diagnosed in Germany (Heidemann et al., 2019), is on statin therapy, the primary goal of our study was to assess direct effects of statin treatment on SARS-CoV-2 infection. Our data suggest that statin treatment does not pose a risk for COVID-19 patients and that the low- to moderate-intensity statin fluvastatin is even associated with a mild attenuation of SARS-CoV-2 infection *in vitro* and *ex vivo*. In accordance, previous retrospective studies reported an amelioration of COVID-19 outcome in patients on statin prescription (Glende et al., 2008; Masana et al., 2020; Tan et al., 2020; Zhang et al., 2020a). However, given the limitations of retrospective studies, placebo-controlled trials are required to clarify the role of statins in COVID-19-infected patients. It is important to note that the inhibitory concentrations observed in our cell culture experiments are an order of magnitude higher than statin serum concentrations in patients and therefore above the moderate intensity therapy dose (80 mg) (Björkhem-Bergman et al., 2011). Based on the studies by Siekmeir et al. and Corsini et al., the tested concentrations would approximately correspond to a therapy dose of 550 mg (10 μM) or 1,600 mg (50 μM) (Corsini et al., 1999; Siekmeier et al., 2001), which suggests that the observed direct effects of statins on SARS-CoV-2 infection in tissue culture may not account for the clinical observations in the

retrospective cohort studies. Unfortunately, fluvastatin, the only statin with anti-coronavirus activity in our study, is prescribed rarely, and only few patients in the retrospective studies received this therapy (Masana et al., 2020; Zhang et al., 2020a). In sum, we found no evidence for a direct aggravating effect of statins on SARS-CoV-2 infection of human lung cells.

In addition to fluvastatin, our initial screen revealed a slight inhibition of HCoV-229E infection by rosuvastatin, pravastatin, and lovastatin (Figure 1A). However, the inhibitory activity of rosuvastatin, the second strongest statin identified, correlated with drug-induced cellular cytotoxicity (Figure 1C). Future research could aim to determine the IC_{50} and CC_{50} for additional potentially antiviral statins. Our study did not include pitavastatin, a lipophilic, well-tolerated statin with a variety of pleotropic effects (Davignon, 2012). Although pitavastatin is a moderate- to low-intensity statin as fluvastatin, dosage is 20–80 times lower (Stone et al., 2014). Therefore, it would be interesting to assess the antiviral activity of pitavastatin against coronaviruses. Of note, chloroquine efficiently inhibited HCoV-229E infection in hepatoma cells but not in respiratory epithelial cells (data not shown); this is in line with findings by Hoffmann and colleagues showing that chloroquine does not inhibit SARS-CoV-2 infection in cells expressing TMPRSS2, including lung epithelial cells (Hoffmann et al., 2020b). Thus, the observed inhibition of HCoV-229E infection in hepatoma cells by chloroquine is likely not physiologically relevant.

The known immunomodulatory effects of statins (Fedson, 2013; Papazian et al., 2013; Pertzov et al., 2019; Sapey et al., 2017) may ameliorate the outcome of hospitalized COVID-19 patients. In our study, statin treatment did not markedly affect SARS-CoV-2 immune sensing or cytokine-mediated cellular responses in comparison to the solvent control (Figure 4). However, the slight upregulation of interferon-stimulated genes (ISGs) in uninfected cells and mild dysregulation of cytokine-regulated genes after infection indicate that fluvastatin may have a relevant immunomodulatory effect on lung epithelial cells, which could ultimately ameliorate COVID-19 immunopathology. Of note, our study does not address the effect of statins on innate immune cells, which may contribute to the clinical observations. In particular, statins have a reported beneficial effect on neutrophil function in infection (Chow et al., 2010; Lee et al., 2013; Sapey et al., 2017) and in pneumonia (Sapey et al., 2019). Investigations on the effect of statins on immune responses and neutrophil function in animal models of COVID-19 are ongoing and will clarify immune-mediated effects of statins.

A possible direct inhibition of the SARS-CoV-2 main protease by statins was postulated in an *in silico* docking study (Reiner et al., 2020). The molecular modeling study predicted similar binding energies for fluvastatin, simvastatin, and rosuvastatin. In our study, however, we observed fluvastatin-specific effects despite using equimolar concentrations of statins. Hence, it is unlikely that direct targeting of the SARS-CoV-2 main protease causes the fluvastatin effects observed here. Alternatively, statins may indirectly inhibit SARS-CoV-2 infection by depleting cholesterol from the plasma membrane. The primary molecular target of statins is HMGCR, a rate-limiting enzyme of the mevalonate pathway that regulates *de novo* cholesterol synthesis (Stancu and Sima, 2001). Therefore, statins may affect SARS-CoV-2 spike-ACE2 receptor interactions due to lipid raft alterations. The latter was previously reported for SARS-CoV (Glende et al., 2008). In line with this, two recent studies state that cholesterol homeostasis is critical for SARS-CoV-2 infection (Daniloski et al., 2021; Wang et al., 2021). In our experimental system we only observed moderate reduction of total cellular cholesterol levels in human lung cells. However, the distribution of cholesterol in the plasma membrane and hence ACE2 receptor localization may nonetheless change upon statin treatment. We are currently investigating the protein interactions of the ACE2 receptor and their cholesterol dependency to shed light on this phenomenon.

Disruption of the mevalonate pathway by statins inhibits dengue, influenza A, and hepatitis C virus replication *in vitro* (Episcopio et al., 2019; Rothwell et al., 2009; Ye et al., 2003). In this study, cholesterol synthesis inhibition did not cause the observed fluvastatin-specific reduction of SARS-CoV-2 infection, because simvastatin, rosuvastatin, and fluvastatin affected cholesterol levels and cholesterol biosynthesis pathway enzyme expression levels in a comparable manner; this suggests that a secondary effect caused the antiviral activity of fluvastatin. Indeed, expanded target spectra of clinically approved drugs have been reported for kinase inhibitors and statins facilitating repurposing of established drugs but also aiding clinical decision-making (Huang et al., 2019; Klaeger et al., 2017). In line with this, statins inhibit human immunodeficiency virus 1 (HIV-1) cell entry by downregulating Rho activity and diminish Ebola virus particle release by interfering with glycoprotein maturation (del Real et al., 2004; Shrivastava-Ranjan et al., 2018).

Interestingly, Zhang et al. showed that fluvastatin, but not pravastatin, interacts with and activates the reactive oxygen species (ROS) scavenging protein peroxiredoxin 1 (PRDX1) (Zhang et al., 2020b). The authors propose that activation of PRDX1 lowers ROS levels and cytokine production and in addition inhibits SARS-CoV-2 infection in cell culture. We showed that fluvastatin specifically downregulated 29 proteins in SARS-CoV-2-infected cells (Figure 5). Interestingly, DDX3X, DDX54, NCL, PRKAR2A, PAPBC1, RAE1, and TUFM are reported interaction partners of SARS-CoV-2 proteins (Cai et al., 2021; Ciccosanti et al., 2021; Gordon et al., 2020; Hui et al., 2021; Schmidt et al., 2021; Zhang et al., 2021), and some of them have been reported to modulate virus infection. For instance, PAPBC1 promotes dengue virus replication (Suzuki et al., 2016) and is cleaved by HIV-1 (Alvarez et al., 2006) and picornaviruses (Rivera and Lloyd, 2008; Zhang et al., 2007). EIF2AK2 and DDX3X are proviral proteins for SARS-CoV-2 (Ciccosanti et al., 2021; Schmidt et al., 2021), porcine reproductive and respiratory syndrome virus (Wang et al., 2016), and hepatitis C virus (Li et al., 2013b; Wang et al., 2016) but inhibit SARS-CoV (de Wilde et al., 2015) by inducing IFN-I responses (Lai et al., 2016). Here, we found that the eukaryotic translation initiation factor 3 subunit B (EIF3B), the RNA-binding component of the eukaryotic translation factor 3 complex (EIF3), is downregulated in fluvastatin-treated infected cells. As EIF3 is critical for the translation of the coronavirus murine hepatitis virus (MHV) (V'kovski et al., 2019), one could speculate that EIF3B is also a host dependency factor for SARS-CoV-2. Interestingly, gene ontology annotation suggests that 80% of proteins downregulated exclusively in fluvastatin-treated SARS-CoV-2-infected cells are targets for posttranslational acetylation. Protein acetylation regulates both cellular and viral protein function, subcellular localization, and interaction (Murray et al., 2019). Whether or not protein acetylation plays a role during SARS-CoV-2 infection requires experimental clarification.

In summary, we observed that fluvastatin downregulates host proteins required for protein translation, DNA damage response, and viral replication. Previous studies underscore the importance of these processes in SARS-CoV-2 infection (Bojkova et al., 2020; Garcia et al., 2021; Gordon et al., 2020; Schmidt et al., 2021; Stukalov et al., 2021). Hence, we propose that fluvastatin exerts secondary effects during SARS-CoV-2 infection by reducing the abundance of SARS-CoV-2 host dependency factors. In order to pinpoint which of the host factors involved in protein translation and viral replication are causing the observed effect, we are currently verifying their biological relevance during SARS-CoV-2 infection. Taken together, cumulative data from this and other studies strongly argue that individuals on statin therapy can safely continue their statin regimen during the current SARS-CoV-2 pandemic and that fluvastatin mitigates SARS-CoV-2 infection in lung epithelial cells by modulating viral replication and translation pathways.

Limitations of the study

Our study suggests a mild effect of fluvastatin on SARS-CoV-2 infection but *in vivo* studies and placebo-controlled clinical trials of clinically relevant concentrations of fluvastatin and other statins are necessary to assess their antiviral effect. Another limitation of our study is the use of SARS-CoV-2 strains isolated early in the pandemic (Wölfel et al., 2020; NCBI #MT093571.1). Even though fluvastatin was efficacious against SARS-CoV-2 infection in all the donor HBECs, virus variants may be differentially sensitive to fluvastatin treatment. Likewise, the antiviral activity of pitavastatin was not evaluated in this study as discussed earlier. Finally, ACE2 was not found by tryptic fingerprinting mass spectrometry, and hence, we could not evaluate whether ACE2 is upregulated upon statin treatment as reported (Li et al., 2013a; Shin et al., 2017). As we did not observe an increase in SARS-CoV-2 infection upon statin treatment, a biologically relevant ACE2 upregulation in our *in vitro* studies seems unlikely. Nevertheless, future complementary omics approaches could strengthen our results, evaluate ACE2 transcript expression levels, and potentially identify additional fluvastatin-specific effects in SARS-CoV-2-infected cells.

STAR★METHODS

Detailed methods are provided in the online version of this paper and include the following:

- KEY RESOURCES TABLE
- RESOURCE AVAILABILITY
  - Lead contact
  - Materials availability
  - Data and code availability
- EXPERIMENTAL MODEL AND SUBJECT DETAILS
  - Cell lines
  - Primary cell cultures

SUPPLEMENTAL INFORMATION

Supplemental information can be found online at https://doi.org/10.1016/j.isci.2021.103469.

ACKNOWLEDGMENTS

G.G. was supported by the Knut and Alice Wallenberg Foundation, the Ministry for Science and Culture of Lower Saxony through the COFONI Fast Track program (#), the Federal Ministry of Education and Research together with the Ministry of Science and Culture of Lower Saxony through the COFONI Fast Track program (#3FT21) and the Professorinnen Programm III, the Deutsche Forschungsgemeinschaft (DFG, German Research Foundation) - Projektnummer 158989968 - SFB 900 project C7, and the Federal Ministry of Education and Research (project COVID-Protect, Projektnummer 01KI20143C). J.K. received funding from the German Academic Exchange Service (DAAD). The work was further funded by the Infection Biology International PhD Program of Hannover Biomedical Research School to R.M., the German Center for Infection Research (DZIF) to A.P.G. and T.P., the Helmholtz Alberta Initiative for Infectious Disease Research (HAI-IDR), the Shandong University Helmholtz International Laboratory to T.P, and the SciLifeLab/KAW national COVID-19 research program project grant 2020 and the Heart- and Lung foundation project grant for COVID-19 (project number 20200385) to A.K.Ö. Virus isolates were received from the European Virus Archive GLOBAL (EVA-GLOBAL) project that has received funding from the European Union's Horizon 2020 research and innovation program under grant agreement No 871029. We acknowledge the Biochemical Imaging Center at Umeå university and the National Microscopy Infrastructure, NMI (VR-RFI 2016-00968) for aiding in microscopy. We thank Anders Blomberg and Gregory Rankin at Umeå University for kindly providing us with lung tissue for isolation of HBECs. We thank Christian Drosten for providing the clinical SARS-CoV-2 isolate, Volker Thiel for the HCoV-229E strain, Sven Reiche for the SARS-CoV-2 reference material used in the real-time qPCR, Yannic Becker for assistance as well as Thomas Schulz, Tommy Olsson, Lars Nyberg, and Anders Sjöstedt for constant support.

AUTHOR CONTRIBUTIONS

G.G and F.J.Z.B. conceptualized the study. F.J.Z.B., R.M., L.L., G.B., M.B, A.K.Ö., E.R., and G.G. developed the methodology. F.J.Z.B., R.M., L.L., G.B., A.P.G., B.C., K.I., J.K., M.B., E.R., A.L., M.v.H., and W.B. carried out investigations. G.G., F.J.Z.B., R.M., L.L., G.B., and M.B. wrote the original draft of the manuscript. Review and editing of the manuscript were carried out by M.B., A.L., K.I., A.K.Ö., E.R., M.v.H., W.B., L.J., A.P.G., G.G., and T.P. G.G., T.P., A.K.Ö., and L.J. acquired funds and provided resources and supervision.

DECLARATION OF INTERESTS

The authors declare no competing interests.

Received: March 17, 2021
Revised: September 8, 2021
Accepted: November 15, 2021
Published: December 17, 2021

REFERENCES

Allegra, A., Di Gioacchino, M., Tonacci, A., Musolino, C., and Gangemi, S. (2020). Immunopathology of SARS-CoV-2 infection: immune cells and Mediators, prognostic factors, and immune-therapeutic implications. Int. J. Mol. Sci. *21*. https://doi.org/10.3390/ijms21134782.

Alvarez, E., Castelló, A., Menéndez-Arias, L., and Carrasco, L. (2006). HIV protease cleaves poly(A)-binding protein. Biochem. J. *396*, 219–226. https://doi.org/10.1042/BJ20060108.

Aviram, M., Dankner, G., Cogan, U., Hochgraf, E., and Brook, J.G. (1992). Lovastatin inhibits low-density lipoprotein oxidation and alters its fluidity and uptake by macrophages: in vitro and in vivo studies. Metab. Clin. Exp. *41*, 229–235. https://doi.org/10.1016/0026-0495(92)90263-a.

Beck, A., Jordan, L.K., Herlitze, S., Amtmann, A., Christian, J., Brogden, G., Adamek, M., Naim, H.Y., and Maria Becker, A. (2018). Quantification of sterols from carp cell lines by using HPLC-MS. Sep. Sci. Plus *1*, 11–21. https://doi.org/10.1002/sscp.201700021.

Björkhem-Bergman, L., Lindh, J.D., and Bergman, P. (2011). What is a relevant statin concentration in cell experiments claiming pleiotropic effects? Br. J. Clin. Pharmacol. *72*, 164–165. https://doi.org/10.1111/j.1365-2125.2011.03907.x.

Blanco-Melo, D., Nilsson-Payant, B.E., Liu, W.-C., Uhl, S., Hoagland, D., Møller, R., Jordan, T.X., Oishi, K., Panis, M., Sachs, D., et al. (2020). Imbalanced host response to SARS-CoV-2 drives development of COVID-19. Cell *181*, 1036–1045.e9. https://doi.org/10.1016/j.cell.2020.04.026.

Bojkova, D., Klann, K., Koch, B., Widera, M., Krause, D., Ciesek, S., Cinatl, J., and Münch, C. (2020). Proteomics of SARS-CoV-2-infected host cells reveals therapy targets. Nature *583*, 469–472. https://doi.org/10.1038/s41586-020-2332-7.

Bonsu, K.O., Reidpath, D.D., and Kadirvelu, A. (2015). Effects of statin treatment on inflammation and cardiac function in heart failure: an adjusted indirect comparison meta-analysis of randomized trials. Cardiovasc. Ther. *33*, 338–346. https://doi.org/10.1111/1755-5922.12150.

Borthwick, F., Mangat, R., Warnakula, S., Jacome-Sosa, M., Vine, D.F., and Proctor, S.D. (2014). Simvastatin treatment upregulates intestinal lipid secretion pathways in a rodent model of the metabolic syndrome. Atherosclerosis *232*, 141–148. https://doi.org/10.1016/j.atherosclerosis.2013.10.031.

Cai, T., Yu, Z., Wang, Z., Liang, C., and Richard, S. (2021). Arginine methylation of SARS-Cov-2 nucleocapsid protein regulates RNA binding, its ability to suppress stress granule formation, and viral replication. J. Biol. Chem. *297*, 100821. https://doi.org/10.1016/j.jbc.2021.100821.

Chow, O.A., von Köckritz-Blickwede, M., Bright, A.T., Hensler, M.E., Zinkernagel, A.S., Cogen, A.L., Gallo, R.L., Monestier, M., Wang, Y., Glass, C.K., and Nizet, V. (2010). Statins enhance formation of phagocyte extracellular traps. Cell Host Microbe *8*, 445–454. https://doi.org/10.1016/j.chom.2010.10.005.

Ciccosanti, F., Di Rienzo, M., Romagnoli, A., Colavita, F., Refolo, G., Castilletti, C., Agrati, C., Brai, A., Manetti, F., Botta, L., et al. (2021). Proteomic analysis identifies the RNA helicase DDX3X as a host target against SARS-CoV-2 infection. Antivir. Res. *190*, 105064. https://doi.org/10.1016/j.antiviral.2021.105064.

Colli, S., Eligini, S., Lalli, M., Camera, M., Paoletti, R., and Tremoli, E. (1997). Vastatins inhibit tissue factor in cultured human macrophages. A novel mechanism of protection against atherothrombosis. Arterioscler. Thromb. Vasc. Biol. *17*, 265–272. https://doi.org/10.1161/01.atv.17.2.265.

Corman, V.M., Landt, O., Kaiser, M., Molenkamp, R., Meijer, A., Chu, D.K., Bleicker, T., Brünink, S., Schneider, J., Schmidt, M.L., et al. (2020). Detection of 2019 novel coronavirus (2019-nCoV) by real-time RT-PCR. Euro Surveill. *25*. https://doi.org/10.2807/1560-7917.ES.2020.25.3.2000045.

Corsini, A., Bellosta, S., Baetta, R., Fumagalli, R., Paoletti, R., and Bernini, F. (1999). New insights into the pharmacodynamic and pharmacokinetic properties of statins. Pharmacol. Ther. *84*, 413–428. https://doi.org/10.1016/s0163-7258(99)00045-5.

Crisby, M., Nordin-Fredriksson, G., Shah, P.K., Yano, J., Zhu, J., and Nilsson, J. (2001). Pravastatin treatment increases collagen content and decreases lipid content, inflammation, metalloproteinases, and cell death in human carotid plaques: implications for plaque stabilization. Circulation *103*, 926–933. https://doi.org/10.1161/01.cir.103.7.926.

Danahay, H., Atherton, H., Jones, G., Bridges, R.J., and Poll, C.T. (2002). Interleukin-13 induces a hypersecretory ion transport phenotype in human bronchial epithelial cells. Am. J. Physiol. Lung Cell Mol. Physiol. *282*, L226–L236. https://doi.org/10.1152/ajplung.00311.2001.

Daniloski, Z., Jordan, T.X., Wessels, H.-H., Hoagland, D.A., Kasela, S., Legut, M., Maniatis, S., Mimitou, E.P., Lu, L., Geller, E., et al. (2021). Identification of required host factors for SARS-CoV-2 infection in human cells. Cell *184*, 92–105.e16. https://doi.org/10.1016/j.cell.2020.10.030.

Davies, N.G., Klepac, P., Liu, Y., Prem, K., Jit, M.; CMMID COVID-19 working group, and Eggo, R.M. (2020). Age-dependent effects in the transmission and control of COVID-19 epidemics. Nat. Med. *26*, 1205–1211. https://doi.org/10.1038/s41591-020-0962-9.

Davignon, J. (2012). Pleiotropic effects of pitavastatin. Br. J. Clin. Pharmacol. *73*, 518–535. https://doi.org/10.1111/j.1365-2125.2011.04139.x.

Episcopio, D., Aminov, S., Benjamin, S., Germain, G., Datan, E., Landazuri, J., Lockshin, R.A., and Zakeri, Z. (2019). Atorvastatin restricts the ability of influenza virus to generate lipid droplets and severely suppresses the replication of the virus. FASEB J. *33*, 9516–9525. https://doi.org/10.1096/fj.201900428RR.

Fedson, D.S. (2013). Treating influenza with statins and other immunomodulatory agents. Antivir. Res *99*, 417–435. https://doi.org/10.1016/j.antiviral.2013.06.018.

Ganjali, S., Bianconi, V., Penson, P.E., Pirro, M., Banach, M., Watts, G.F., and Sahebkar, A. (2020). Commentary: statins, COVID-19, and coronary artery disease: killing two birds with one stone. Metab. Clin. Exp. *113*, 154375. https://doi.org/10.1016/j.metabol.2020.154375.

Garcia, G., Sharma, A., Ramaiah, A., Sen, C., Purkayastha, A., Kohn, D.B., Parcells, M.S., Beck, S., Kim, H., Bakowski, M.A., et al. (2021). Antiviral drug screen identifies DNA-damage response inhibitor as potent blocker of SARS-CoV-2 replication. Cell Rep. *35*, 108940. https://doi.org/10.1016/j.celrep.2021.108940.

Glende, J., Schwegmann-Wessels, C., Al-Falah, M., Pfefferle, S., Qu, X., Deng, H., Drosten, C., Naim, H.Y., and Herrler, G. (2008). Importance of cholesterol-rich membrane microdomains in the interaction of the S protein of SARS-coronavirus with the cellular receptor angiotensin-converting enzyme 2. Virology *381*, 215–221. https://doi.org/10.1016/j.virol.2008.08.026.

Gordon, D.E., Jang, G.M., Bouhaddou, M., Xu, J., Obernier, K., White, K.M., O'Meara, M.J., Rezelj, V.V., Guo, J.Z., Swaney, D.L., et al. (2020). A SARS-CoV-2 protein interaction map reveals targets for drug repurposing. Nature *583*, 459–468. https://doi.org/10.1038/s41586-020-2286-9.

Gu, Q., Paulose-Ram, R., Burt, V.L., and Kit, B.K. (2014). Prescription cholesterol-lowering medication use in adults aged 40 and over: United States, 2003-2012. NCHS Data Brief *177*, 1–8.

Gupta, A., Madhavan, M.V., Poterucha, T.J., DeFilippis, E.M., Hennessey, J.A., Redfors, B., Eckhardt, C., Bikdeli, B., Platt, J., Nalbandian, A., et al. (2021). Association between antecedent statin use and decreased mortality in hospitalized patients with COVID-19. Nat. Commun. *12*, 1325. https://doi.org/10.1038/s41467-021-21553-1.

Heidemann, C., Du, Y., Baumert, J., Paprott, R., and Lampert, T. (2019). Soziale Ungleichheit und Diabetes mellitus – Zeitliche Entwicklungbei Erwachsenen in Deutschland. J. Health Monitor. *4*, Robert Koch-Institut.

Hoffmann, M., Kleine-Weber, H., Schroeder, S., Krüger, N., Herrler, T., Erichsen, S., Schiergens, T.S., Herrler, G., Wu, N.-H., Nitsche, A., et al. (2020a). SARS-CoV-2 cell entry depends on ACE2 and TMPRSS2 and is blocked by a clinically proven protease inhibitor. Cell *181*, 271–280.e8. https://doi.org/10.1016/j.cell.2020.02.052.

Hoffmann, M., Mösbauer, K., Hofmann-Winkler, H., Kaul, A., Kleine-Weber, H., Krüger, N., Gassen, N.C., Müller, M.A., Drosten, C., and Pöhlmann, S. (2020b). Chloroquine does not inhibit infection of human lung cells with SARS-CoV-2. Nature *585*, 588–590. https://doi.org/10.1038/s41586-020-2575-3.

Huang, Y., Furuno, M., Arakawa, T., Takizawa, S., de Hoon, M., Suzuki, H., and Arner, E. (2019). A framework for identification of on- and off-target transcriptional responses to drug treatment. Sci. Rep. *9*, 17603. https://doi.org/10.1038/s41598-019-54180-4.

Hui, K.P.Y., Cheung, M.-C., Perera, R.A.P.M., Ng, K.-C., Bui, C.H.T., Ho, J.C.W., Ng, M.M.T., Kuok, D.I.T., Shih, K.C., Tsao, S.-W., et al. (2020). Tropism, replication competence, and innate immune responses of the coronavirus SARS-CoV-2 in human respiratory tract and conjunctiva: an analysis in ex-vivo and in-vitro cultures. Lancet Respir. Med. *8*, 687–695. https://doi.org/10.1016/S2213-2600(20)30193-4.

Hui, X., Zhang, L., Cao, L., Huang, K., Zhao, Y., Zhang, Y., Chen, X., Lin, X., Chen, M., and Jin, M. (2021). SARS-CoV-2 promote autophagy to suppress type I interferon response. Signal Transduct. Target. Ther. *6*, 180. https://doi.org/10.1038/s41392-021-00574-8.

Klaeger, S., Heinzlmeir, S., Wilhelm, M., Polzer, H., Vick, B., Koenig, P.-A., Reinecke, M., Ruprecht, B., Petzoldt, S., Meng, C., et al. (2017). The target landscape of clinical kinase drugs. Science *358*. https://doi.org/10.1126/science.aan4368.

Radenkovic, D., Chawla, S., Pirro, M., Sahebkar, A., and Banach, M. (2020). Cholesterol in relation to COVID-19: should we care about it? J. Clin. Med. *9*, 1909. https://doi.org/10.3390/jcm9061909.

Raivo Kolde. (2019). pheatmap:Pretty Heatmaps. Rpackage version 1.0.12. https://CRAN.R-project.org/package=pheatmap.

Krämer, A., Green, J., Pollard, J., and Tugendreich, S. (2014). Causal analysis approaches in ingenuity pathway analysis. Bioinformatics *30*, 523–530. https://doi.org/10.1093/bioinformatics/btt703.

Lai, M.-C., Sun, H.S., Wang, S.-W., and Tarn, W.-Y. (2016). DDX3 functions in antiviral innate immunity through translational control of PACT. FEBS J. *283*, 88–101. https://doi.org/10.1111/febs.13553.

Laufs, U., La Fata, V., Plutzky, J., and Liao, J.K. (1998). Upregulation of endothelial nitric oxide synthase by HMG CoA reductase inhibitors. Circulation *97*, 1129–1135. https://doi.org/10.1161/01.cir.97.12.1129.

Lee, C.S., Yi, E.H., Lee, J.-K., Won, C., Lee, Y.J., Shin, M.K., Yang, Y.M., Chung, M.-H., Lee, J.W., Sung, S.-H., and Ye, S.-K. (2013). Simvastatin suppresses RANTES-mediated neutrophilia in polyinosinic-polycytidylic acid-induced pneumonia. Eur. Respir. J. *41*, 1147–1156. https://doi.org/10.1183/09031936.00050612.

Li, G.-M., Li, Y.-G., Yamate, M., Li, S.-M., and Ikuta, K. (2007). Lipid rafts play an important role in the early stage of severe acute respiratory syndrome-coronavirus life cycle. Microbes Infect. *9*, 96–102. https://doi.org/10.1016/j.micinf.2006.10.015.

Li, Y.-H., Wang, Q.-X., Zhou, J.-W., Chu, X.-M., Man, Y.-L., Liu, P., Ren, B.-B., Sun, T.-R., and An, Y. (2013a). Effects of rosuvastatin on expression of angiotensin-converting enzyme 2 after vascular balloon injury in rats. J. Geriatr. Cardiol. *10*, 151–158. https://doi.org/10.3969/j.issn.1671-5411.2013.02.009.

Li, Q., Pène, V., Krishnamurthy, S., Cha, H., and Liang, T.J. (2013b). Hepatitis C virus infection activates an innate pathway involving IKK-α in lipogenesis and viral assembly. Nat. Med. *19*, 722–729. https://doi.org/10.1038/nm.3190.

Liao, J.K., and Laufs, U. (2005). Pleiotropic effects of statins. Annu. Rev. Pharmacol. Toxicol. *45*, 89–118. https://doi.org/10.1146/annurev.pharmtox.45.120403.095748.

Lu, Y., Liu, D.X., and Tam, J.P. (2008). Lipid rafts are involved in SARS-CoV entry into Vero E6 cells. Biochem. Biophys. Res. Commun. *369*, 344–349. https://doi.org/10.1016/j.bbrc.2008.02.023.

Masana, L., Correig, E., Rodríguez-Borjabad, C., Anoro, E., Arroyo, J.A., Jericó, C., Pedragosa, A., Miret, M.Ia, Näf, S., Pardo, A., et al. (2020). Effect of statin therapy on SARS-CoV-2 infection-related mortality in hospitalized patients. Eur. Heart J. Cardiovasc. Pharmacother. https://doi.org/10.1093/ehjcvp/pvaa128.

Merico, D., Isserlin, R., Stueker, O., Emili, A., and Bader, G.D. (2010). Enrichment map: a network-based method for gene-set enrichment visualization and interpretation. PLoS One *5*, e13984. https://doi.org/10.1371/journal.pone.0013984.

Mitacchione, G., Schiavone, M., Curnis, A., Arca, M., Antinori, S., Gasperetti, A., Mascioli, G., Severino, P., Sabato, F., Caracciolo, M.M., et al. (2021). Impact of prior statin use on clinical outcomes in COVID-19 patients: data from tertiary referral hospitals during COVID-19 pandemic in Italy. J. Clin. Lipidol. *15*, 68–78. https://doi.org/10.1016/j.jacl.2020.12.008.

Murray, L.A., Combs, A.N., Rekapalli, P., and Cristea, I.M. (2019). Methods for characterizing protein acetylation during viral infection. Meth. Enzymol. *626*, 587–620. https://doi.org/10.1016/bs.mie.2019.06.030.

Oesterle, A., Laufs, U., and Liao, J.K. (2017). Pleiotropic effects of statins on the cardiovascular system. Circ. Res. *120*, 229–243. https://doi.org/10.1161/CIRCRESAHA.116.308537.

Papazian, L., Roch, A., Charles, P.-E., Penot-Ragon, C., Perrin, G., Roulier, P., Goutorbe, P., Lefrant, J.-Y., Wiramus, S., Jung, B., et al.; STATIN-VAP Study Group (2013). Effect of statin therapy on mortality in patients with ventilator-associated pneumonia: a randomized clinical trial. JAMA *310*, 1692–1700. https://doi.org/10.1001/jama.2013.280031.

Parsamanesh, N., Karami-Zarandi, M., Banach, M., Penson, P.E., and Sahebkar, A. (2021). Effects of statins on myocarditis: a review of underlying molecular mechanisms. Prog. Cardiovasc. Dis. https://doi.org/10.1016/j.pcad.2021.02.008.

Perez-Riverol, Y., Csordas, A., Bai, J., Bernal-Llinares, M., Hewapathirana, S., Kundu, D.J., Inuganti, A., Griss, J., Mayer, G., Eisenacher, M., et al. (2019). The PRIDE database and related tools and resources in 2019: improving support for quantification data. Nucleic Acids Res. *47*, D442–D450. https://doi.org/10.1093/nar/gky1106.

Pertzov, B., Eliakim-Raz, N., Atamna, H., Trestioreanu, A.Z., Yahav, D., and Leibovici, L. (2019). Hydroxymethylglutaryl-CoA reductase inhibitors (statins) for the treatment of sepsis in adults - a systematic review and meta-analysis. Clin. Microbiol. Infect. *25*, 280–289. https://doi.org/10.1016/j.cmi.2018.11.003.

Price-Haywood, E.G., Burton, J., Fort, D., and Seoane, L. (2020). Hospitalization and mortality among black patients and white patients with Covid-19. N. Engl. J. Med. *382*, 2534–2543. https://doi.org/10.1056/NEJMsa2011686.

R Core Team (2020). R: A Language and Environment for Statistical Computing (R Foundation for Statistical Computing). https://www.R-project.org/.

Ravindra, N.G., Alfajaro, M.M., Gasque, V., Habet, V., Wei, J., Filler, R.B., Huston, N.C., Wan, H., Szigeti-Buck, K., Wang, B., et al. (2020). Single-cell longitudinal analysis of SARS-CoV-2 infection in human bronchial epithelial cells. BioRxiv. https://doi.org/10.1101/2020.05.06.081695.

Del Real, G., Jiménez-Baranda, S., Mira, E., Lacalle, R.A., Lucas, P., Gómez-Moutón, C., Alegret, M., Peña, J.M., Rodríguez-Zapata, M., Alvarez-Mon, M., et al. (2004). Statins inhibit HIV-1 infection by down-regulating Rho activity. J. Exp. Med. *200*, 541–547. https://doi.org/10.1084/jem.20040061.

Reiner, Ž., Hatamipour, M., Banach, M., Pirro, M., Al-Rasadi, K., Jamialahmadi, T., Radenkovic, D., Montecucco, F., and Sahebkar, A. (2020). Statins and the COVID-19 main protease: in silico evidence on direct interaction. Arch. Med. Sci. *16*, 490–496. https://doi.org/10.5114/aoms.2020.94655.

Rivera, C.I., and Lloyd, R.E. (2008). Modulation of enteroviral proteinase cleavage of poly(A)-binding protein (PABP) by conformation and PABP-associated factors. Virology *375*, 59–72. https://doi.org/10.1016/j.virol.2008.02.002.

Rosendal, E., Wigren, J., Groening, R., Yongdae, K., Nilsson, E., Sharma, A., Espaillat, A., Hanke, L., Thunberg, T., McInerney, G., et al. (2020). Detection of asymptomatic SARS-CoV-2 exposed individuals by a sensitive S-based ELISA. medRxiv. https://doi.org/10.1101/2020.06.02.20120477.

Rothwell, C., Lebreton, A., Young Ng, C., Lim, J.Y.H., Liu, W., Vasudevan, S., Labow, M., Gu, F., and Gaither, L.A. (2009). Cholesterol biosynthesis modulation regulates dengue viral replication. Virology *389*, 8–19. https://doi.org/10.1016/j.virol.2009.03.025.

Sapey, E., Patel, J.M., Greenwood, H.L., Walton, G.M., Hazeldine, J., Sadhra, C., Parekh, D., Dancer, R.C.A., Nightingale, P., Lord, J.M., and Thickett, D.R. (2017). Pulmonary infections in the elderly lead to impaired neutrophil targeting, which is improved by simvastatin. Am. J. Respir. Crit. Care Med. *196*, 1325–1336. https://doi.org/10.1164/rccm.201704-0814OC.

Sapey, E., Patel, J.M., Greenwood, H., Walton, G.M., Grudzinska, F., Parekh, D., Mahida, R.Y., Dancer, R.C.A., Lugg, S.T., Howells, P.A., et al. (2019). Simvastatin improves neutrophil function and clinical outcomes in pneumonia. A pilot randomized controlled clinical trial. Am. J. Respir. Crit. Care Med. *200*, 1282–1293. https://doi.org/10.1164/rccm.201812-2328OC.

Schindelin, J., Arganda-Carreras, I., Frise, E., Kaynig, V., Longair, M., Pietzsch, T., Preibisch, S., Rueden, C., Saalfeld, S., Schmid, B., et al. (2012). Fiji: an open-source platform for biological-image analysis. Nat. Methods *9*, 676–682. https://doi.org/10.1038/nmeth.2019.

Schmidt, N., Lareau, C.A., Keshishian, H., Ganskih, S., Schneider, C., Hennig, T., Melanson, R., Werner, S., Wei, Y., Zimmer, M., et al. (2021). The SARS-CoV-2 RNA-protein interactome in infected human cells. Nat. Microbiol. *6*, 339–353. https://doi.org/10.1038/s41564-020-00846-z.

Shin, Y.H., Min, J.J., Lee, J.-H., Kim, E.-H., Kim, G.E., Kim, M.H., Lee, J.J., and Ahn, H.J. (2017). The effect of fluvastatin on cardiac fibrosis and angiotensin-converting enzyme-2 expression in glucose-controlled diabetic rat hearts. Heart Vessels *32*, 618–627. https://doi.org/10.1007/s00380-016-0936-5.

Shrivastava-Ranjan, P., Flint, M., Bergeron, É., McElroy, A.K., Chatterjee, P., Albariño, C.G., Nichol, S.T., and Spiropoulou, C.F. (2018). Statins suppress Ebola virus infectivity by interfering with glycoprotein processing. MBio *9*. https://doi.org/10.1128/mBio.00660-18.

Siekmeier, R., Lattke, P., Mix, C., Park, J.W., and Jaross, W. (2001). Dose dependency of fluvastatin pharmacokinetics in serum determined by reversed phase HPLC. J. Cardiovasc. Pharmacol. Ther. *6*, 137–145. https://doi.org/10.1177/107424840100600205.

Kamil Slowikowski. (2020). grepel: Automatically PositionNon-Overlapping Text Labels with "gplot2". R package version 0.8.2. https://CRAN.R-project.org/package=ggrepel.

Stancu, C., and Sima, A. (2001). Statins: mechanism of action and effects. J. Cell Mol. Med. *5*, 378–387. https://doi.org/10.1111/j.1582-4934.2001.tb00172.x.

Stone, N.J., Robinson, J.G., Lichtenstein, A.H., Bairey Merz, C.N., Blum, C.B., Eckel, R.H., Goldberg, A.C., Gordon, D., Levy, D., Lloyd-Jones, D.M., et al. (2014). 2013 ACC/AHA guideline on the treatment of blood cholesterol to reduce atherosclerotic cardiovascular risk in adults: a report of the American college of cardiology/American Heart association task force on practice guidelines. J. Am. Coll. Cardiol. *63*, 2889–2934. https://doi.org/10.1016/j.jacc.2013.11.002.

Stukalov, A., Girault, V., Grass, V., Karayel, O., Bergant, V., Urban, C., Haas, D.A., Huang, Y., Oubraham, L., Wang, A., et al. (2021). Multilevel proteomics reveals host perturbations by SARS-CoV-2 and SARS-CoV. Nature *594*, 246–252. https://doi.org/10.1038/s41586-021-03493-4.

Suzuki, Y., Chin, W.-X., Han, Q., Ichiyama, K., Lee, C.H., Eyo, Z.W., Ebina, H., Takahashi, H., Takahashi, C., Tan, B.H., et al. (2016). Characterization of RyDEN (C19orf66) as an interferon-stimulated cellular inhibitor against dengue virus replication. Plos Pathog. *12*, e1005357. https://doi.org/10.1371/journal.ppat.1005357.

Tan, W.Y.T., Young, B.E., Lye, D.C., Chew, D.E.K., and Dalan, R. (2020). Statin use is associated with lower disease severity in COVID-19 infection. Sci. Rep. *10*, 17458. https://doi.org/10.1038/s41598-020-74492-0.

Tyanova, S., Temu, T., and Cox, J. (2016). The MaxQuant computational platform for mass spectrometry-based shotgun proteomics. Nat. Protoc. *11*, 2301–2319. https://doi.org/10.1038/nprot.2016.136.

Vincent, M.J., Bergeron, E., Benjannet, S., Erickson, B.R., Rollin, P.E., Ksiazek, T.G., Seidah, N.G., and Nichol, S.T. (2005). Chloroquine is a potent inhibitor of SARS coronavirus infection and spread. Virol. J. *2*, 69. https://doi.org/10.1186/1743-422X-2-69.

V'kovski, P., Gerber, M., Kelly, J., Pfaender, S., Ebert, N., Braga Lagache, S., Simillion, C., Portmann, J., Stalder, H., Gaschen, V., et al. (2019). Determination of host proteins composing the microenvironment of coronavirus replicase complexes by proximity-labeling. Elife *8*. https://doi.org/10.7554/eLife.42037.

Wang, X., Zhang, H., Abel, A.M., and Nelson, E. (2016). Protein kinase R (PKR) plays a pro-viral role in porcine reproductive and respiratory syndrome virus (PRRSV) replication by modulating viral gene transcription. Arch. Virol. *161*, 327–333. https://doi.org/10.1007/s00705-015-2671-0.

Wang, M., Cao, R., Zhang, L., Yang, X., Liu, J., Xu, M., Shi, Z., Hu, Z., Zhong, W., and Xiao, G. (2020). Remdesivir and chloroquine effectively inhibit the recently emerged novel coronavirus (2019-nCoV) in vitro. Cell Res. *30*, 269–271. https://doi.org/10.1038/s41422-020-0282-0.

Wang, R., Simoneau, C.R., Kulsuptrakul, J., Bouhaddou, M., Travisano, K.A., Hayashi, J.M., Carlson-Stevermer, J., Zengel, J.R., Richards, C.M., Fozouni, P., et al. (2021). Genetic screens identify host factors for SARS-CoV-2 and common cold coronaviruses. Cell *184*, 106–119.e14. https://doi.org/10.1016/j.cell.2020.12.004.

Wassmann, S., Laufs, U., Bäumer, A.T., Müller, K., Ahlbory, K., Linz, W., Itter, G., Rösen, R., Böhm, M., and Nickenig, G. (2001). HMG-CoA reductase inhibitors improve endothelial dysfunction in normocholesterolemic hypertension via reduced production of reactive oxygen species. Hypertension *37*, 1450–1457. https://doi.org/10.1161/01.hyp.37.6.1450.

Wickham, H., Averick, M., Bryan, J., Chang, W., McGowan, L., François, R., Grolemund, G., Hayes, A., Henry, L., Hester, J., et al. (2019). Welcome to the tidyverse. JOSS *4*, 1686. https://doi.org/10.21105/joss.01686.

de Wilde, A.H., Wannee, K.F., Scholte, F.E.M., Goeman, J.J., Ten Dijke, P., Snijder, E.J., Kikkert, M., and van Hemert, M.J. (2015). A kinome-wide small interfering RNA screen identifies proviral and antiviral host factors in severe acute respiratory syndrome coronavirus replication, including double-stranded RNA-activated protein kinase and early secretory pathway proteins. J. Virol. *89*, 8318–8333. https://doi.org/10.1128/JVI.01029-15.

Wölfel, R., Corman, V.M., Guggemos, W., Seilmaier, M., Zange, S., Müller, M.A., Niemeyer, D., Jones, T.C., Vollmar, P., Rothe, C., et al. (2020). Virological assessment of hospitalized patients with COVID-2019. Nature *581*, 465–469. https://doi.org/10.1038/s41586-020-2196-x.

World Health Organization. (2020). Coronavirus Disease (COVID-19) Pandemic. https://www.who.int/emergencies/diseases/novel-coronavirus-2019.

Ye, J., Wang, C., Sumpter, R., Brown, M.S., Goldstein, J.L., and Gale, M. (2003). Disruption of hepatitis C virus RNA replication through inhibition of host protein geranylgeranylation. Proc. Natl. Acad. Sci. USA *100*, 15865–15870. https://doi.org/10.1073/pnas.2237238100.

Zhang, B., Morace, G., Gauss-Müller, V., and Kusov, Y. (2007). Poly(A) binding protein, C-terminally truncated by the hepatitis A virus proteinase 3C, inhibits viral translation. Nucleic Acids Res. *35*, 5975–5984. https://doi.org/10.1093/nar/gkm645.

Zhang, X.-J., Qin, J.-J., Cheng, X., Shen, L., Zhao, Y.-C., Yuan, Y., Lei, F., Chen, M.-M., Yang, H., Bai, L., et al. (2020a). In-hospital use of statins is associated with a reduced risk of mortality among individuals with COVID-19. Cell Metab. *32*, 176–187.e4. https://doi.org/10.1016/j.cmet.2020.06.015.

Zhang, H., Shen, J., Xu, H., Sun, J., Yin, W., Zuo, Y., Wang, Z., Xiong, F., Zhang, Y., Lin, H., et al. (2020b). Activation of peroxiredoxin 1 by fluvastatin effectively protects from inflammation and SARS-CoV-2. SSRN J. https://doi.org/10.2139/ssrn.3606782.

Zhang, K., Miorin, L., Makio, T., Dehghan, I., Gao, S., Xie, Y., Zhong, H., Esparza, M., Kehrer, T., Kumar, A., et al. (2021). Nsp1 protein of SARS-CoV-2 disrupts the mRNA export machinery to inhibit host gene expression. Sci. Adv. *7*, eabe7386. https://doi.org/10.1126/sciadv.abe7386.

STAR★METHODS

KEY RESOURCES TABLE

REAGENT or RESOURCE	SOURCE	IDENTIFIER
Antibodies		
SARS-CoV-2 (nucleocapsid)	SinoBiological	40143-R001; RRID:AB_2827974
mucin5AC (clone 45M1)	ThermoFisher	MS-145-P; RRID:AB_62731
acetylated tubulin	Sigma	T6793; RRID:AB_477585
Goat anti-rabbit AF488	ThermoFisher	A11008; RRID:AB_143165
Goat anti-mouse A647	ThermoFisher	A-21240; RRID:AB_141658
Goat anti-mouse AF568	ThermoFisher	A-21144; RRID:AB_2535780
Bacterial and virus strains		
HCoV-229E	Volker Thiel (Universität Bern)	NA
SARS-CoV-2	Christian Drosten (Charité, Berlin) through the European Virus Archive – Global (EVAg)	SARS-CoV-2/München-1.2/2020/984,p3
SARS-CoV-2 (ALI experiment)	GeneBank	SARS-CoV-2/01/human/2020/SWE
		GeneBank accession no. MT093571.1
Chemicals, peptides, and recombinant proteins		
Hoechst33342	ThermoFisher	62249
Fluvastatin	Sigma	SML0038
Simvastatin	Sigma	S6196
Atorvastatin	Sigma	PZ0001
Lovastatin	Sigma	M2147
Pravastatin	biomol	Cay-10010342
Rosuvastatin	Sigma	SML1264
Chloroquine	Sigma	C6628
MTT reagent (3-[4,5-dimethylthiazol-2-yl]-2,5 diphenyltetrazolium bromide	invitrogen	M6494
Critical commercial assays		
NucleoSpin RNA kit	Macherey-Nagel	740955.250
QIAamp Viral RNA Mini Kit	Qiagen	52906
SuperScript™ III One-Step RT-PCR System with Platinum™ Taq DNA Polymerase	invitrogen	12574026
PrimeScript™ RT Master Mix	Takara	RR036A
TB Green® Premix Ex Taq™	Takara	RR82LR
qPCRBIO Probe 1-Step Go master mix	PCR Biosystems	PB25.41-03
Deposited data		
mass spectrometry proteomics data	ProteomeXchange	ProteomeXchange: PXD023422
Experimental models: Cell lines		
HEK293T	ATCC	CRL-3612
Huh7.5 FLuc	kindly provided by Charles M. Rice (Rockefeller Institute, NY, US)	NA
Calu-3	kindly provided by Stefan Pöhlmann (German Primate Center, Göttingen, Germany).	ATCC-HTB-55

(*Continued on next page*)

Continued

REAGENT or RESOURCE	SOURCE	IDENTIFIER
Vero	ATCC	CCL-81
Vero E6	ATCC	CRL-1586
Experimental models: Organisms/strains		
Primary human bronchial epithelial cells	Patient derived (University hospital of Umeå, Sweden)	NA
Oligonucleotides		
RFC2 primer set: CCAGCAAGCCTTGAGGAGAAC, GGCTCGATGATCTTATCCGAAG	Microsynth	NA
HMGA2 primer set: ACCCAGGGGAAGACCCAAA, CCTCTTGGCCGTTTTTCTCCA	Microsynth	NA
NCL primer set: GAACCGACTACGGCTTTCAAT, AGCAAAAACATCGCTGATACCA	Microsynth	NA
ß-actin primer set: CAC CAT TGG CAA TGA GCG GTT C, AGG TCT TTG CGG ATG TCC ACG T	Microsynth	NA
SARS-CoV-2 primer and probe: fv: GTGARATGGTCATGTGTGGCGG, rv: CARATGTTAAASACACTATTAGCATA, probe: FAM-CAGGTGGAACCTCATCAGGAGATGC-BBQ	TIB MOLBIOL	NA
SARS-CoV-2 primer and probe (ALI experiment): fv: GTCATGTGTGGCGGTTCACT, rv: CAACACTATTAGCATAAGCAGTTG T, probe: CAGGTGGAACCTCATCAGGAGATGC	Eurofins genomics	NA
Software and algorithms		
Peaks X+	Bioinformatics Solutions	https://www.bioinfor.com/peaks-studio-x-plus/
MaxQuant (1.6.17.0)	MaxQuant	https://www.maxquant.org/
R (4.0.2)	R Foundation	https://www.R-project.org/
STRING	STRING Consortium	https://string-db.org/
Cytoscape 3.8.2	Cytoscape Consortium	https://cytoscape.org/
BioRender	BioRender	https://biorender.com/
GraphPad Prism8	GraphPad	https://www.graphpad.com/scientific-software/prism/

RESOURCE AVAILABILITY

Lead contact

Further information and requests for resources and reagents should be directed to and will be fulfilled by the lead contact, Gisa Gerold (gisa.gerold@tiho-hannover.de).

Materials availability

This study did not generate new unique reagents.

Data and code availability

All data reported in this paper will be shared by the lead contact upon request. The mass spectrometry proteomics data have been deposited to the ProteomeXchange Consortium via the PRIDE (Perez-Riverol et al., 2019) partner repository with the dataset identifier PXD023422.

This paper does not report original code.

Any additional information required to reanalyze the data reported in this paper is available from the lead contact upon request.

EXPERIMENTAL MODEL AND SUBJECT DETAILS

Cell lines

HEK293T cells, Huh7.5 cells constitutively expressing a Firefly luciferase (Huh7.5 Fluc) and Calu-3 cells were maintained in DMEM supplemented with 10% fetal bovine serum, 2 mM glutamine, 0.1 mM non-essential amino acids and 1% Penicillin/Streptomycin at 37°C and 5% CO_2.

Primary cell cultures

Primary human bronchial epithelial cells (HBEC) were isolated with informed consent from lung tissue from three individual patients, who underwent thoracic surgery at the University hospital of Umeå, Sweden, with ethical permission approved by the local Ethics Review Board. HBEC were grown in Bronchial Epithelial Cell Medium (BEpiCM, SC3211-b, SienCell) with recommended supplements (SC3262, SienCell) and 100 U/ml penicillin +100 μg/ml streptomycin (PeSt; Thermo Fisher Scientific). For differentiation, 150.000 cells were seeded onto a 12 mm semipermeable transwell insert (0.4 μm Pore Polyester Membrane Insert, Corning) in differentiation media (DMEM:BEpiCM 1:1 supplemented with 52 μg/ml bovine pituitary extract, 0.5 μg/ml hydrocortisone, 0.5 ng/ml human recombinant epidermal growth factor, 0.5 μg/ml epinephrine, 10 μg/ml transferrin, 5 μg/ml insulin, 50 nM retinoic acid (all from Sigma Aldrich) and PeSt (Danahay et al., 2002). Cells were maintained submerged for the first 7 days, after which the media was removed from the apical side and cells were grown at air-liquid interface for an additional two weeks to reach full differentiation. Media was replaced trice/week with addition of fresh retinoic acid to the media shortly before usage. Differentiation of the HBEC were assessed using light microscopy focusing on epithelial morphology, presence of ciliated cells, and mucus production. Presence of ciliated cells and goblet cells was also determined with IF using antibodies directed against acetylated-tubulin and muc5AC, respectively, as described under IF staining below.

METHOD DETAILS

Virus strains

The recombinant HCoV-229E encoding a Renilla luciferase gene was produced in Huh7.5 cells at 33°C and titrated on Huh7.5 cells. The SARS-CoV-2 isolate (strain SARS-CoV-2/München-1.2/2020/984,p3) was kindly provided by Christian Drosten (Charité, Berlin) through the European Virus Archive – Global (EVAg) and used for cell culture assays including experiments used for MS. The SARS-CoV-2 patient isolate SARS-CoV-2/01/human/2020/SWE; GeneBank accession no. MT093571.1 was provided by the Public Health Agency of Sweden and used for the infection of ALI cultures. Both strains were amplified in Vero cells and handled under BSL3 conditions.

Reagents and inhibitors

Fluvastatin (Sigma, order no. SML0038), simvastatin (Sigma, order no. S6196), atorvastatin (Sigma, order no. PZ0001), lovastatin (Sigma, order no. M2147), pravastatin (biomol, Cay-10010342) and rosuvastatin (Sigma, order no. SML1264) were dissolved in DMSO. Chloroquine (Sigma, C6628), dissolved in H_2O, served as a positive control.

Effect of statins on HCoV-229E

Huh7.5 Fluc cells were seeded in 96-well plates at a density of $1x10^4$ cells/well in complete Dulbecco's Modified Eagle's Medium (DMEM) and incubated for 24 h at 37°C (5% CO_2). The cells were pretreated for 24 h with either 5 μM of each compound or serial dilutions of the tested compounds in 100 μl final volume. Following the pretreatment, cells were inoculated with HCoV-229E at MOI 0.005 in the presence of the tested compounds. The inoculum was removed 4 h later and fresh medium containing the respective compounds was added. Cells were lysed 48 h post inoculation in 50 μl detergent containing buffer and Renilla luciferase activity, as a measurement for infection, was determined by mixing 20 μl of lysate with 60 μl of luciferase substrate solution (Coelenterazine, 0.42 mg/ml in methanol). To determine cell viability, Firefly luciferase activity was measured from the same lysate by adding D-luciferin (0.2 mM D-luciferin in 25 mM glycyl-glycine) as a substrate. Luciferase activity was measured in a Centro XS3 LB960 (Berthold Technologies) microplate reader.

SARS-2 infection and quantification by RT-qPCR

For infection experiments with SARS-CoV-2, the SARS-CoV-2 isolate (strain SARS-CoV-2/München-1.2/2020/984,p3) (Wölfel et al., 2020), kindly provided by Christian Drosten (Charité, Berlin) through the

European Virus Archive – Global (EVAg), was propagated in Vero cells (3 passages) after primary isolation from patient material. For infection, Calu-3 cells were seeded in collagen coated 24 well plates at a density of $4.5x10^5$ cells/well for initial infection studies or in 6 well plates at a density of $2x10^6$ cells/well for the MS data set. Cells were pretreated with 10 μM fluvastatin, simvastatin, rosuvastatin or DMSO for 24 h and then infected with SARS-CoV-2 isolate at MOI $2.0x10^{-5}$ based on titration in Vero cells. Heat-inactivated virus was used as a control to determine unspecific binding of virions and RNA. 4 h post infection, the inoculum was removed, cells were washed twice with PBS and fresh medium containing the respective compound was added. The infection was stopped 48 h later, viral RNA was isolated from cell lysates and supernatants using NucleoSpin RNA kit (Macherey-Nagel) and QIAamp Viral RNA Mini Kit (Qiagen), respectively, following the manufacturer's instructions. RT-qPCR was performed in duplicates using Superscript III one step RT-PCR system with Platinum Taq Polymerase (Invitrogen) according to the manufacturer's instructions. The following primers and probe were used: SARS-CoV-2 fv: GTGARATGGTCATGTGTGGCGG, rv: CARATGTTAAASACACTATTAGCATA, probe: FAM-CAGGTGGAACCTCATCAGGAGATGC-BBQ (TIB MOLBIOL). The thermal cycling conditions were performed using a LightCycler 480 (Roche) as follows: 55°C for 10 min for reverse transcription, followed by 95°C for 3 min and then 45 cycles of 95°C for 15 s and 58°C for 30 s (Corman et al., 2020). Viral copy numbers were determined using a standard calibrated against a reference standard provided by Sven Reiche (FLI, Germany). In addition, SARS-CoV-2 titer in cell culture supernatants was quantified by $TCID_{50}$ assay on Vero cells. Therefore, Vero cells were seeded in 96 well plates and incubated with serial dilutions of cell culture supernatant. 72 h later, cells were fixed with 10% formalin and stained with crystal violet.

Quantification of host gene expression by qPCR

Transcript levels of host factors were determined in total cellular RNA isolated from SARS-CoV-2 infected cells (see above). To this end, 500 ng of extracted total RNA were reverse transcribed into cDNA using PrimeScript™ RT Master Mix (Takara) according to the manufacturer's instructions. The cDNA was subsequently used in qPCR using SYBR TB Green® Premix Ex Taq™ (Takara). Primers were obtained from Harvard Primer Bank and β-actin was used as a housekeeping gene.

Cell viability assay

Cell viability was determined at the end of the experiment either by measuring Firefly luciferase activity in cell lysates (Huh7.5 Fluc cells) or by MTT assay. For the latter, MTT reagent (3-[4,5-dimethylthiazol-2-yl]-2,5 diphenyltetrazolium bromide, 0.5 mg/mL in medium) was added to the cells. The reaction was stopped with DMSO after 1 h and optical density was measured at 570 nm using a plate reader (Synergy 2, BioTek®).

Virus production for ALI infection

SARS-CoV-2 patient isolate SARS-CoV-2/01/human/2020/SWE; GeneBank accession no. MT093571.1 was provided by the Public Health Agency of Sweden. The isolate was propagated in Vero E6 cells for 48 h and titrated by plaque assay (Rosendal et al., 2020). For the plaque assay, 10-fold serial dilutions were added to Vero E6 cells ($4*10^5$/well) seeded in 12-well plates (VWR) 12-24 h prior to infection. After 1 h incubation, the inoculum was removed, and wells were overlayed with semisolid DMEM + 2 % FBS + PeSt + 1.2 % Avicel RC/CL for incubation at 37°C in 5% CO_2. At 65 h.p.i., the semisolid overlay was removed, and cells were fixed with 4% formaldehyde for 30 min. Cells were washed with PBS and stained with 0.5% crystal violet in 20% MeOH for 5 minutes. Plates were washed with water and the plaques counted.

Infection of ALI cultures and sample collection

For pretreatment at 24 h prior to infection, the medium in the basal chambers were replaced with medium containing either carrier control (DMSO), 10 μM or 50 μM fluvastatin. Immediately prior to infection, basal medium containing drug or carrier control was replaced again and the apical side of the HBEC ALI cultures was rinsed three times with PBS. For infection, $4.5x10^4$ PFU of SARS-CoV-2 (SARS-CoV-2/01/human/2020/SWE; GeneBank accession no. MT093571.1) in a total volume of 300 μl infection medium (DMEM + 10 U PeSt) was added to the apical compartment. Cells were incubated at 37°C and 5% CO_2 for 3 h before the inoculum was removed and the cells washed one more time with PBS.

At 24, 48 and 72 h.p.i., produced and secreted virus was collected by addition of 300 μl infection medium to the apical chamber and incubation at 37°C and 5% CO_2 for 1 h. 100 μl of the sample was used for RNA extraction using Qiaamp Viral RNA mini kit (Qiagen) according to the manufacturer''s instructions. At

48 h.p.i., the medium in the basolateral chamber was replaced with fresh medium containing drug or carrier control. After sample collection from the apical side at 72 h.p.i., the cells were washed three times with PBS and fixed over night at 4°C in 4% formaldehyde.

Real-time qPCR for the quantification of virus RNA in supernatant

To quantify the viral genome in the supernatant, extracted RNA was used as template in qPCRBIO Probe 1-Step Go master mix (PCR Biosystems, London, UK) together with SARS-CoV-2 primers (Forward: GTC ATG TGT GGC GGT TCA CT, Reverse: CAA CAC TAT TAG CAT AAG CAG TTG T) and probe (CAG GTG GAA CCT CAT CAG GAG ATG C) specific for viral RdRp (Corman et al., 2020). Forward and reverse primer were modified by Magnus Lindh at Sahlgrenska University Hospital, Gothenburg. Viral copy numbers were determined by calibration against a reference standard provided by Sven Reiche (FLI, Germany). A standard curve ranging from 1 to 1 × 10^6 genomes was run together with the SARS CoV-2 samples. The qPCR reaction was carried out with the StepOnePlus™ Real-Time PCR system (Thermo Fischer, Waltham, MA, USA).

Immunofluorescence analysis

HBEC ALI inserts were washed thrice apically and basally for 10 min with IF buffer (130 mM NaCl, 10 mM Na_2HPO_4/NaH_2PO_4, 0.05% NaN_3, 0.1% BSA, 0.2% Triton X-100, 0.04% Tween-20, pH7.4). Inserts were blocked for 1 h at room temperature and subsequently incubated with primary antibodies (SARS: SARS-CoV-2: nucleocapsid, 40143-R001, SinoBiological; mucin5AC: Ab-1 (45M1), #MS-145-P, ThermoFisher; acetylated tubulin: T6793-0.2 ml, Sigma; 1:200) overnight at 4°C in IF buffer + 10% FBS. ALI inserts were washed thrice apically and basally for 20 min with IF buffer and subsequently stained with the respective secondary antibodies (AF488: ThermoFisher A11088; AF568: ThermoFisher A21144; AF647: ThermoFisher A21240; 1:200) and Hoechst33342 (ThermoFisher 62249; 1:10000) for 1 h at room temperature in IF buffer + 10% FBS. Before imaging, samples were washed thrice apically and basally for 20 min with IF buffer and rinsed twice apically and basally for 50 min with PBS.

Quantification

For overview pictures and quantification, whole inserts were imaged on a Cytation5 imaging platform (BioTek®) with installed DAPI, GFP and Cy5 LED/filter cube setups by taking 4x4 images with a 10% overlap for stitching with a 4x objective and subsequent image stitching based on the DAPI channel using linear blend fusion (Gen5 prime software, BioTek®). Total fluorescence intensity was quantified on a plug (region of interest) covering the maximal insert surface without touching the rim for each of the channels (Gen5 prime, BioTek®).

Confocal imaging

At two sites, 4 mm punches (biopsy puncher, Miltex 33-34) were taken from the whole insert and mounted on cytoslides (Shandon, ThermoFisher 5991057) on ProLong Gold antifade mounting medium (ThermoFisher, P10144). Images were acquired on a Leica SP8 confocal microscope with a 63x oil objective at the BICU imaging unit of Umeå University. Representative sites were imaged as z-stacks of 40 slices with 0.5 μm step size and converted by maximum intensity projection using Fiji (Schindelin et al., 2012).

Mass spectrometry

Calu-3 cells were treated with statins and infected as described in section 'SARS-2 infection and quantification by RT-qPCR'. Cells were lysed in buffer containing 4% SDS, 10 mM DTT and 10 mM HEPES (pH 8), heated at 95°C for 10 min and sonicated at 4°C for 15 min (level 5, Bioruptor, Diagenode). Proteins were precipitated with acetone at −20°C and resuspended in 8 M urea buffer containing 10 mM HEPES (pH 8). Total protein was diluted to a final concentration of 100 μg/ml in 10 mM HEPES (pH 8) and 2 μg total protein was used for further analysis. Reduction was performed by applying a final concentration of 5 mM TCEP and heating at 55°C for 1 h, alkylation was then performed by the addition of final concentration of 20 mM MMTS and incubation for 10 min at room temperature. Protein digestion was performed by adding trypsin at a final concentration of 1 μg protease to 50 μg total protein and incubation over night at 37°C while shaking. Peptide recovery was performed using EvoTips (Evosep) and eluted using 0.2% TFA in 60% acetonitrile (ACN). Peptides were dried and suspended in 100 μl 0.1% FA. Twenty percent of the samples were loaded on Evotips.

Samples were injected into an Evosep I HPLC (Evosep) connected to a timsTOFPro mass spectrometer with PASEF (Bruker). The 15 sample per day standard method (EvoSep I HPLC), and the standard Bruker method "PASEF method for short gradients" (MS/MS timsTOFPro) were applied.

MS/MS raw data files were processed by using Peaks X+ (Bioinformatics Solutions) and MaxQuant (1.6.17.0) software (Tyanova et al., 2016) and UniProtKB databases (Homo sapiens: UP000005640/April 28, 2020; SARS-CoV-2: UP000464024/September 29, 2020). The following search parameters were used: enzyme, trypsin; maximum missed cleavages, 2; fixed modifications, methyl methanethiosulfonate (composition of H2CS at cysteine); variable modifications, oxidation (M) and acetyl (protein N-term); peptide tolerance, 20 ppm; LFQ min. ratio count, 1; Match between runs Alignment time window, 10 min; other parameters are used as default settings. Data acquisition and analyses were performed in R (4.0.2) ("R Core Team (2020). R: A language and environment for statistical computing. R Foundation for Statistical Computing, Vienna, Austria.," n.d.) using following packages; tidyverse (Wickham et al., 2019), ggrepel (Slowikowski, 2020) and pheatmap (Raivo Kolde, 2019). All the data were transformed into log2 values and proteins with at least one valid value were used for further analysis. The missing values in each sample were replaced with a lower normal distribution (downshift = 1.8, standard deviation = 0.3). P-values from Student's t-tests and differences of log2 values were used for the generation of volcano plots. Protein-protein interaction network analysis of statistically dysregulated proteins (p-value cut-off = 0.05) was performed with STRING with a medium confidence threshold (0.4). STRING analysis was exported to Cytoscape 3.8.2 and enrichment analysis executed with EnrichmentMap 3.1.0 plugin (Merico et al., 2010). Pathway and upstream regulator analyses were generated through the use of Ingenuity Pathway Analysis (Krämer et al., 2014).

Cholesterol analysis

Calu-3 cells were seeded on 24 well plates precoated with collagen. 24 h post seeding, cells were treated in duplicate with 10 μM of each statin in medium with or without FCS for two days. The cells were then washed twice in PBS, counted and stored in 1 ml HPLC-grade water. Samples for lipid isolation were dissolved in methanol:acetonitrile (1:1) and quantified using a Hitachi Chromaster HPLC system fitted with a VDSpher PUR C18-H (3 μm, 150×2.0 mm) column (VDS Optilab, Berlin, Germany) (Beck et al., 2018). The following separation conditions were used; The mobile phase consisted of methanol:acetonitire (1:1, v/v) and 0.1% formic acid dissolved in H2O (95:5), at a flow rate of 0.2 ml/min, a column temperature of 22°C and the UV detector set at 202 nm.

QUANTIFICATION AND STATISTICAL ANALYSIS

Experiments were conducted in three biological replicates each with three technical replicates unless otherwise stated in the figure legends. All statistical analyses were performed using one or two-way analysis of variance (ANOVA) followed by Dunnett or Sidak's multiple comparison test as stated in the figure legends using GraphPad Prism software version 8 (San Diego, CA, USA).